Geologic Setting of PACManus Hydrothermal Vent Fields – High-resolution mapping and in situ observations.

Janis Thal[1*], Maurice Tivey[2], Dana Yoerger[2], Niels Jöns[1], Wolfgang Bach[1]

[1]*MARUM, University of Bremen, 28359 Bremen, Germany*
[2]*Woods Hole Oceanographic Institution, Woods Hole, MA02543, USA*

**corresponding author: ja_th@uni-bremen.de, phone: (+49) 421-218-46405*

Abstract

This study presents a systematic analysis and interpretation of autonomous underwater vehicle-based microbathymetry combined with remotely operated vehicle (ROV) video recordings, rock analyses and temperature measurements within the PACManus hydrothermal area located on Pual Ridge in the Bismarck Sea of eastern Manus Basin. The data obtained during research cruise Magellan-06 and So-216 provides a framework for understanding the relationship between the volcanism, tectonism and hydrothermal activity. PACManus is a submarine felsic vocanically-hosted hydrothermal area that hosts multiple vent fields located within several hundred meters of one another but with different fluid chemistries, vent temperatures and morphologies. The total area of hydrothermal activity is estimated to be 20,279 m2. The microbathymetry maps combined with the ROV video observations allow for precise high-resolution mapping estimates of the areal extents of hydrothermal activity. We find the distribution of hydrothermal fields in the PACManus area is primarily controlled by volcanic features that include lava domes, thick and massive blocky lava flows, breccias and feeder dykes. Spatial variation in the permeability of local volcanic facies appears to control the distribution of venting within a field. We define a three-stage chronological sequence for the volcanic evolution of the PACManus based on lava flow morphology, sediment cover and lava SiO2 concentration. In Stage-1, sparsely to moderately porphyritic dacite lavas (68 - 69.8 wt. % SiO2) erupted to form domes or cryptodomes. In Stage-2, aphyric lava with slightly lower SiO2 concentrations (67.2 – 67.9 wt. % SiO2) formed jumbled and pillowed lava flows. In the most recent phase Stage-3, massive blocky lavas with 69 to 72.5 wt. % SiO2 were erupted through multiple vents constructing a volcanic ridge identified as the PACManus neovolcanic zone. The transition between these stages may be gradual and related to progressive heating of a silicic magma following a recharge event of hot, mantle-derived melts.

Keywords: PACManus; submarine volcanism, Manus Basin, hydrothermal vent, ROV, black smoker

1. Introduction

Hydrothermal systems at ridges dominated by felsic volcanism are not as well studied as the more widely documented hydrothermal systems of basalt-hosted mid-ocean ridge (MOR) spreading centres (e.g. de Ronde et al., 2001; German et al., 2004). Subaqueous, felsic volcanic ridges are common in immature back-arc basins with volatile-rich magmas, whose genesis is strongly influenced by processes related to nearby subduction zones (Kamenetsky et al., 2001; Martinez and Taylor, 2003; Park et al., 2009). It is well known the felsic host rock composition combined with the magmatic, volatile-enriched hydrothermal fluids play an important role in enriching economically important metals such as copper, gold and zinc in the vent deposits (e.g. Sangster, 1980; Herzig, 1999; Iizasa, 1999; Hannington et al., 2005, 2011; Mosier et al., 2009). The surface expressions of submarine felsic-hosted hydrothermal systems (i.e. hydrothermal areas) are potentially important analogues for many ore-deposits found on land today. The PACManus (Papua – Australia – Canada – Manus) hydrothermal area is one of these surface expressions located on the crest of the Pual Ridge in the eastern Manus Basin, an immature back-arc basin (Fig. 1).

This study presents a systematic analysis using a Geographical Information Systems (GIS) database of autonomous underwater vehicle (AUV) based microbathymetry combined with remotely-operated vehicle (ROV) video recordings, rock analyses and temperature measurements of individual hydrothermal discharge sites for the hydrothermal fields of the PACManus hydrothermal area in the SE Manus Basin. It allows documentation of the first detailed, georeferenced mapping of the volcanic and hydrothermal structures in the PACManus hydrothermal area. Our analysis of the data has resulted in a set of comprehensive maps of the geological structures of the PACManus hydrothermal area and documents the interaction between subaqueous felsic volcanism and its influence on hydrothermal fluid discharge at the seafloor.

2. Geological setting

The Manus Basin is located in the eastern part of the Bismarck Sea, which is situated in the western Pacific Ocean northeast of the Papua New Guinea mainland (Fig. 1). Manus Basin, with an average water depth of 2000 m, is an oblique opening back-arc basin formed by the northward subduction of the Solomon Sea Plate along the New Britain Trench (Taylor, 1979; Martinez and Taylor, 1996, 2003; Lee and Ruellan, 2006). Crustal extension in the Manus Basin is distributed between the Manus Spreading Centre (MSC), the Manus Extensional Transform Zone (METZ), the Southern Rifts (SR) and the Southeast Ridges (SER; Martinez and Taylor, 1996). The clockwise rotation (~ 8° Ma-1) of the South Bismarck Plate around a pole at 10.2ºN, 33.3ºW (Star in Fig.1) causes asymmetric spreading of the North and South Bismarck Plate (Tregoning et al., 1999). This is manifest by spreading rates of 137.5 mm a-1 at the SER, which are the highest spreading rates within the Bismarck Sea (Tregoning, 2002). The SER region also has bimodal, basaltic to rhyolitic volcanism (Binns and Scott, 1993), which is typical of the initial opening phase of a back-arc-basin.

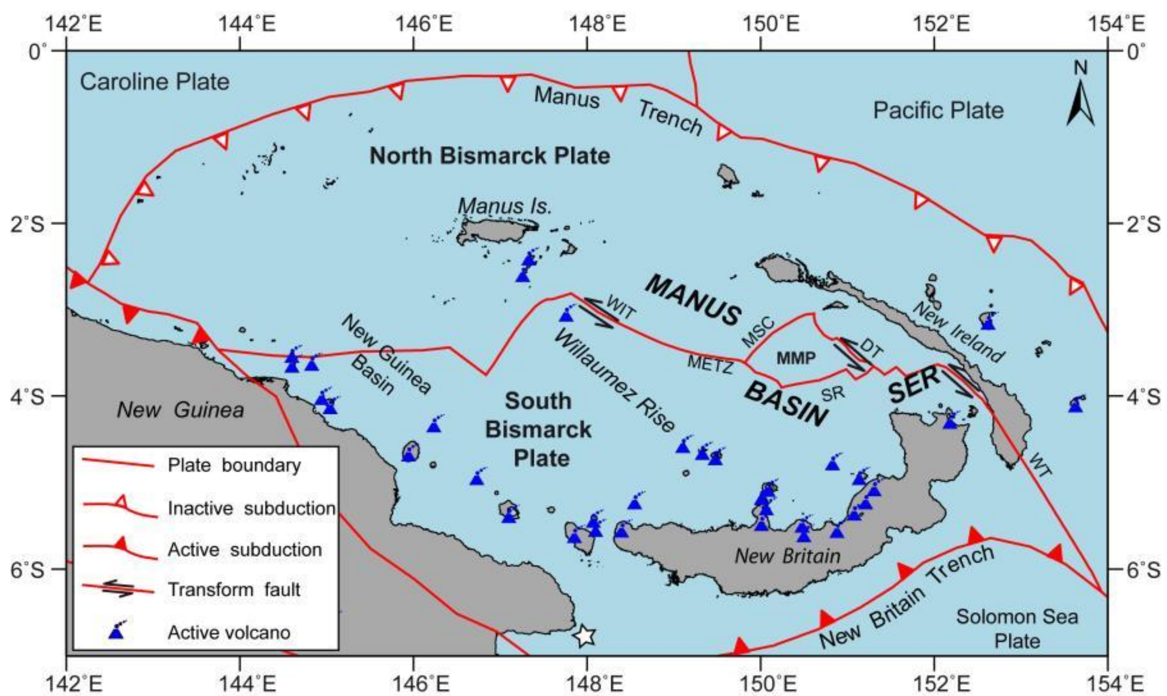

Fig. 1: Tectonics at the Manus Basin. Abbreviations: WT = Weitin Transform; DT = Djaul Transform; WIT = Willaumez Transform; METZ = Manus Extensional Transform Zone; SR = Southern Ridges; MMP = Manus Microplate; SER = Southeast Ridges; MSC = Manus Spreading Centre; Star = Absolute Pole of South Bismarck Plate Rotation; Plate boundaries from Bird (2003).

The SER region is a rift zone of pre-existing island arc crust, which consists of a series of sigmoidally-shaped volcanic ridges influenced by the strike-slip movement generated by the two bordering left lateral transform faults; the Weitin Transform (WT) and the Djaul Transform (DT) (Taylor et al., 1994) (Figs. 1, 2; supplemental video S3). The PACManus hydrothermal area lies on the central crest of Pual Ridge, which is part of the SER. Pual ridge is ~20 km long, 1 - 1.5 km wide and rises 500 – 600 m above the surrounding seafloor (Fig. 2; Binns and Scott, 1993; Bartetzko et al., 2003; Paulick et al., 2004). The summit of Pual Ridge is capped by a 200 m by

800 m long central neovolcanic zone. The AUV ABE collected a comprehensive microbathymetry map of the PACManus hydrothermal area, which provides sub-meter scale resolution and delineates several volcanic edifices 200-300 m across with steep-sided flow fronts exhibiting crenulated margins (Figs. 3, 4).

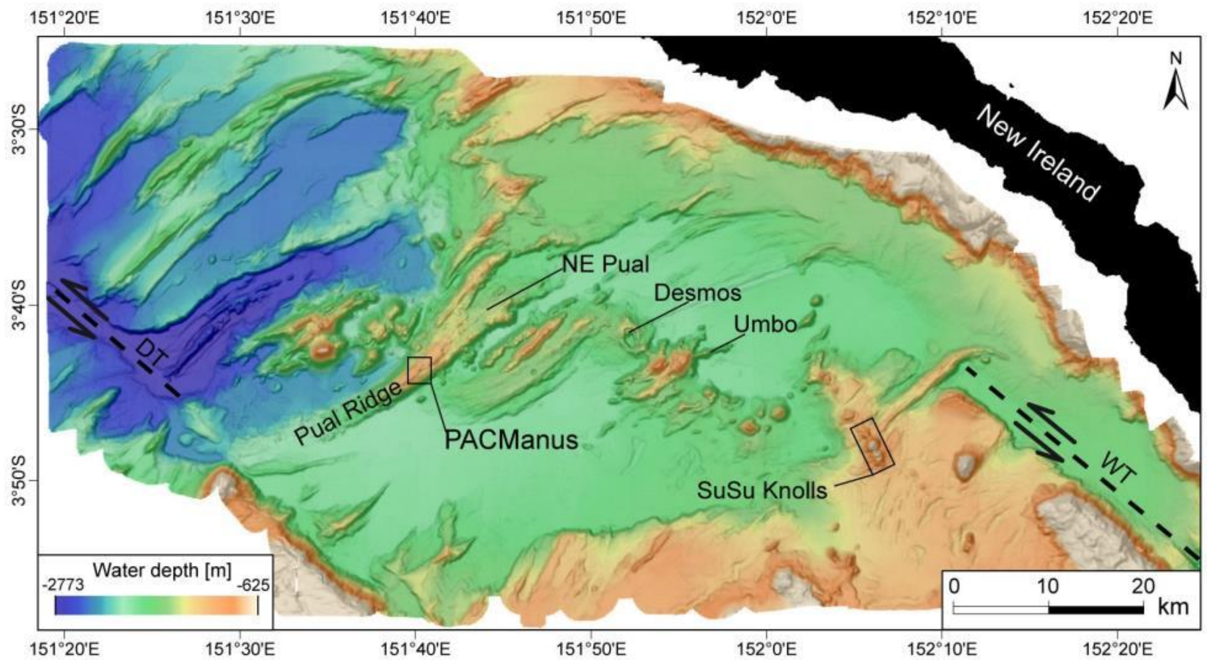

Fig. 2: Multibeam bathymetry map of South Eastern Ridges (SER) region in the Eastern Manus Basin region with known hydrothermal area. WT = Weitin Transform; DJ = Djaul Transform. Data recorded on BAMBUS – RV Sonne 216 cruise.

2.1 PACManus Hydrothermal District (3°43.5' S - 151°40.5' E)

The PACManus (Papua – Australia – Canada – Manus) hydrothermal area on the crest of Pual Ridge, at a water depth around 1640 – 1740 m, is the most active of the known hydrothermal areas of the SER region. PACManus hydrothermal area hosts several hydrothermal fields, each up to 100 – 200 m in diameter. From south to north the fields are identified as follows: Tsukushi, Snowcap, Fenway (and adjacent Mimosa and Solwara-8), Satanic Mills, Roman Ruins, and Roger's Ruins (and adjacent Solwara-6 and Solwara-7; Fig. 10).

The PACManus hydrothermal area was first discovered on the PACManus-1 expedition in 1991 when a first assessment of the distribution and size of the hydrothermal deposits was conducted (Binns and Scott, 1993).

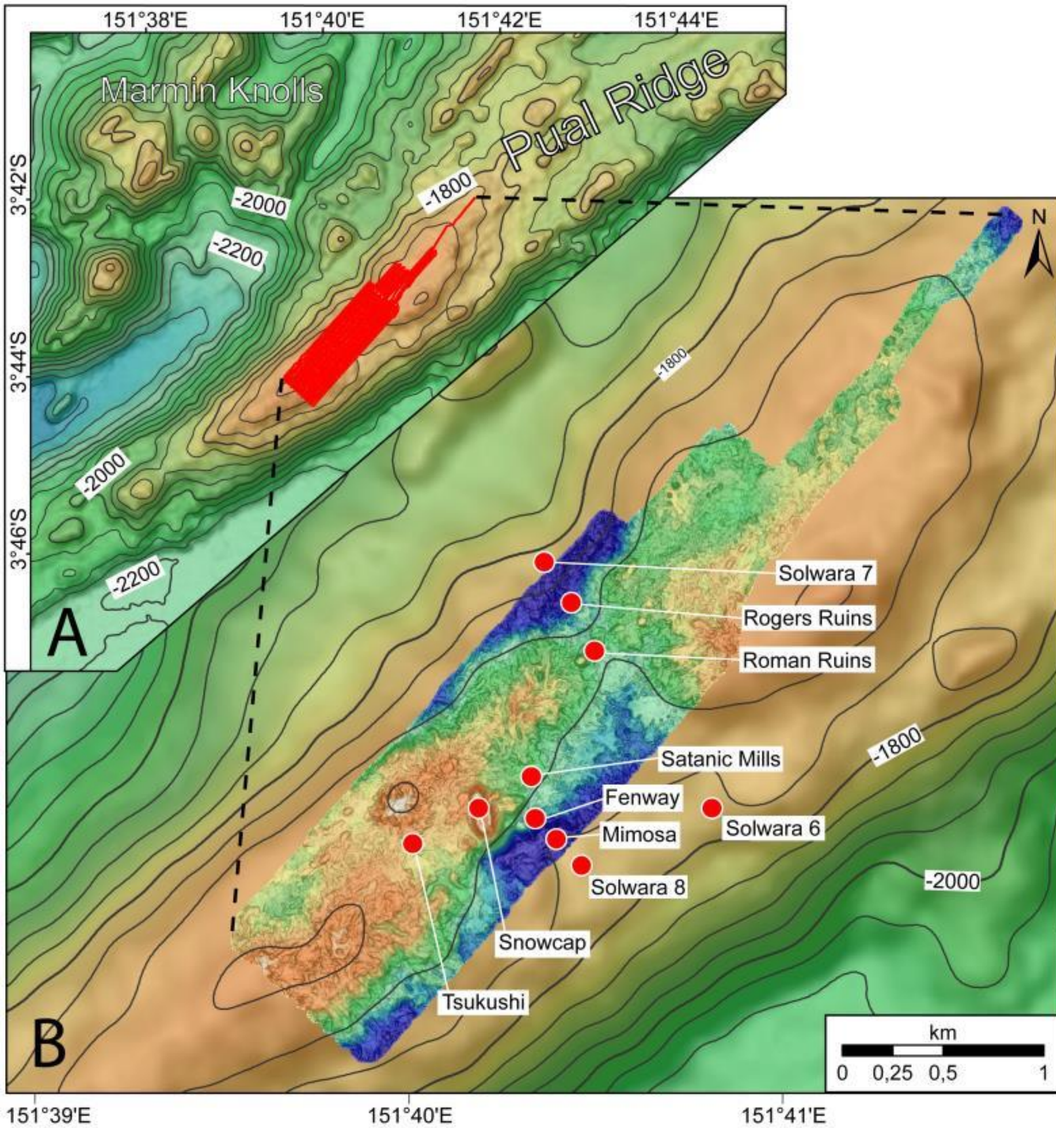

Fig. 3a+b: Red lines in fig. 3a indicate trackline coverage of AUV ABE high resolution multibeam mapping surveys. Figure 3b shows detailed AUV ABE multibeam bathymetry map of Pual Ridge with the primary PACManus hydrothermal fields. Background bathymetry source: BAMBUS - RV Sonne 216 cruise.

This discovery was followed by 13 international research cruises to the region to study various aspects of the hydrothermal fields including the detailed bathymetry, magnetics, hydrothermal fluid chemistry, biology, hydrothermal vent deposit mineralogy, host rock lithology and composition and overall geologic structure of Pual Ridge (e.g. Binns and Scott, 1993; Auzende et al., 1996, 2000; Gamo et al., 1997; Hashimoto et al., 1999; Petersen et al., 2005; Tivey et al., 2006; Binns et al., 2007; Craddock and Bach, 2010; Bach et al., 2011; Reeves et al., 2011).

In 2000, the Ocean Drilling Programm (ODP) Leg 193 drilling expedition provided subsurface information on the volcanic facies present at three of the PACManus hydrothermal vent fields.

The PACManus ODP drilling program resulted in holes penetrating between 100 and 380 m deep into the crust of the Snowcap and Roman Ruins areas and 20 mbsf at Satanic Mills (Binns et al., 2007).

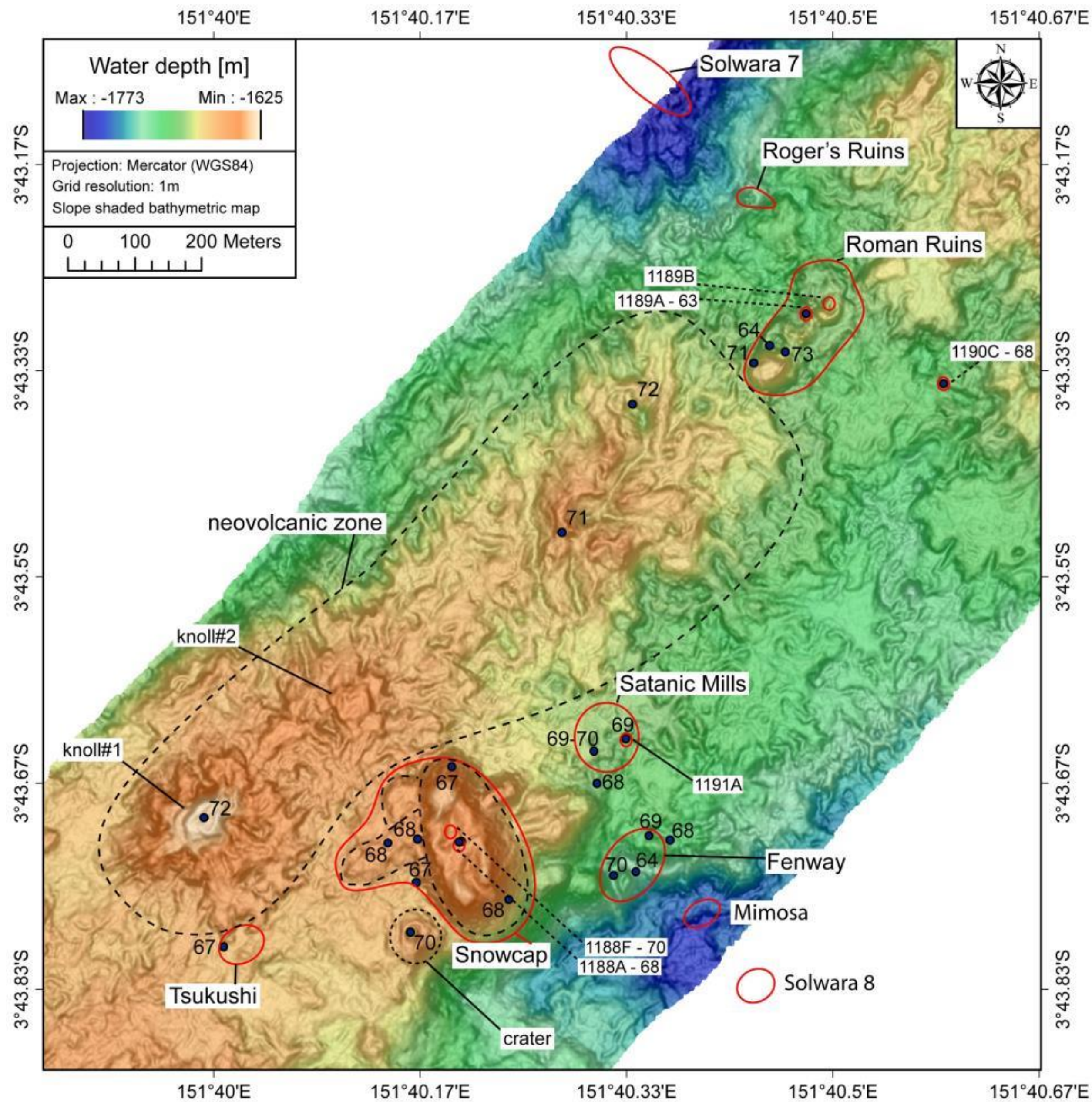

Fig. 4: Overview of PACManus with all hydrothermal discharge sites (except Solwara 6), major morphological features and rock sample locations with SiO_2 concentration (wt. %).

Another drilling campaign in 2002 sampled the shallow seafloor to fill in the gap caused by the requirement to case the upper parts of the holes during ODP Leg 193 operations (Petersen et al., 2005). The lateral distribution of the recovered volcanic units was unknown at the time of drilling and could only be speculated on as being proximal versus distal volcanic facies based on recovered samples and borehole imagery of volcanic facies (Bartetzko et al., 2003; Paulick et al., 2004). Major questions remained as to the geological context of the vent fields and the distribution of fluid flow following the completion of the drilling campaigns (Binns et al., 2007).

Although the hydrothermal fields of PACManus are within hundreds of meters of each other, their fluids have different temperatures, varying chemical compositions (Reeves et al., 2011) and plume particle colours that range from clear to grey to black. In areas of chronic vent fluid discharge, biological communities are well-developed, including bacterial mats, molluscs, tube worms, crabs, anemones, holothurians, and a range of crustaceans and fish (Hashimoto et al., 1999).

3. Methods

During Woods Hole Oceanographic Institution's RV Melville cruise Magellan-06 in 2006, ship-based multibeam bathymetry was complemented by high-resolution AUV ABE bathymetry mapping along with 10 ROV Jason-2 dives (208-216, 222) that collected rock as well as hydrothermal fluid and sulphide samples. A total of 3 ABE dives (188, 190, 191) focused on the PACManus summit area of Pual Ridge (Fig. 3). A follow-up cruise with RV Sonne (SO-216) in June/July of 2011 used the ROV MARUM Quest to record additional seafloor video images and collect fluids, rocks and biota. This cruise allowed confirmation of the previous mapping and assessment of potential temporal changes in activity.

For this study, we analysed video data from 20 ROV dives and coregistered the information with the microbathymetry map recorded by AUV ABE. Further information on data acquisition and processing methods is available in the appendix A1.

Analysis of rock compositions, fluid sample chemistry (Reeves et al., 2011), sulphide chimney compositions (Craddock et al., 2010) as well as fluid temperatures aid our interpretations. Rock sample compositions reported in this paper (Table S1, supplementary) were analysed with a JXA 8900 R Electron Probe Microanalyser at the Christian-Albrechts-Universität zu Kiel.

A Geographical Information System (GIS) was used to correlate and coregister the available map and video data and to superimpose different volcanic facies, hydrothermal deposit observations, and sediment cover identified from the videos onto the microbathymetry basemap.

3.1 Seafloor volcanic morphology

We use the terminology for volcanic morphology based on definitions from McPhie et al. (1993). In general, the direction of lava movement was determined from flow structures on the surface of lava flows observed in the video data. The sediment thickness in areas without hydrothermal activity was used as a crude proxy for the relative age of volcanic events. For regions with a very thick sediment cover, the unit “single outcrops” was used, because an identification of the underlying lava structure was not possible. We have grouped volcaniclastics, breccias and pumice together and mapped it as breccia. Based on visual criteria, the volcanic seafloor was mapped as blocky lava (for irregular, angular and blocky structures) and pillow lava. Some volcanic flow units have surface structures intermediate between those of pillow and blocky lava, including slabby and jumbled lava. They are mapped as “mixed lava” that often also comprises various lava flow morphologies, such as blocky lava with pillowed subdomains. An example is the large lava field between two of the vent fields (Tsukushi and Snowcap) in the southern part of the PACManus hydrothermal area (Fig. 5). Sulphide chimney clusters were mapped as “active” when they showed focused fluid discharge through orifices in chimneys. In the absence of discrete venting, the smokers were mapped as “inactive”. Shimmering water and the occurrence of vent-related fauna was used to identify diffuse discharge. Taxonomic differentiation of the biological communities was beyond the scope of this research.

Other types of deposits at discharge sites, such as elemental sulphur or oxides, were also identified and mapped. At Fenway hydrothermal field, irregularly-shaped anhydrite deposits are abundant and we mapped these as separate units. Lava flow fronts are only depicted where a sudden and obvious change in the lithology was encountered.

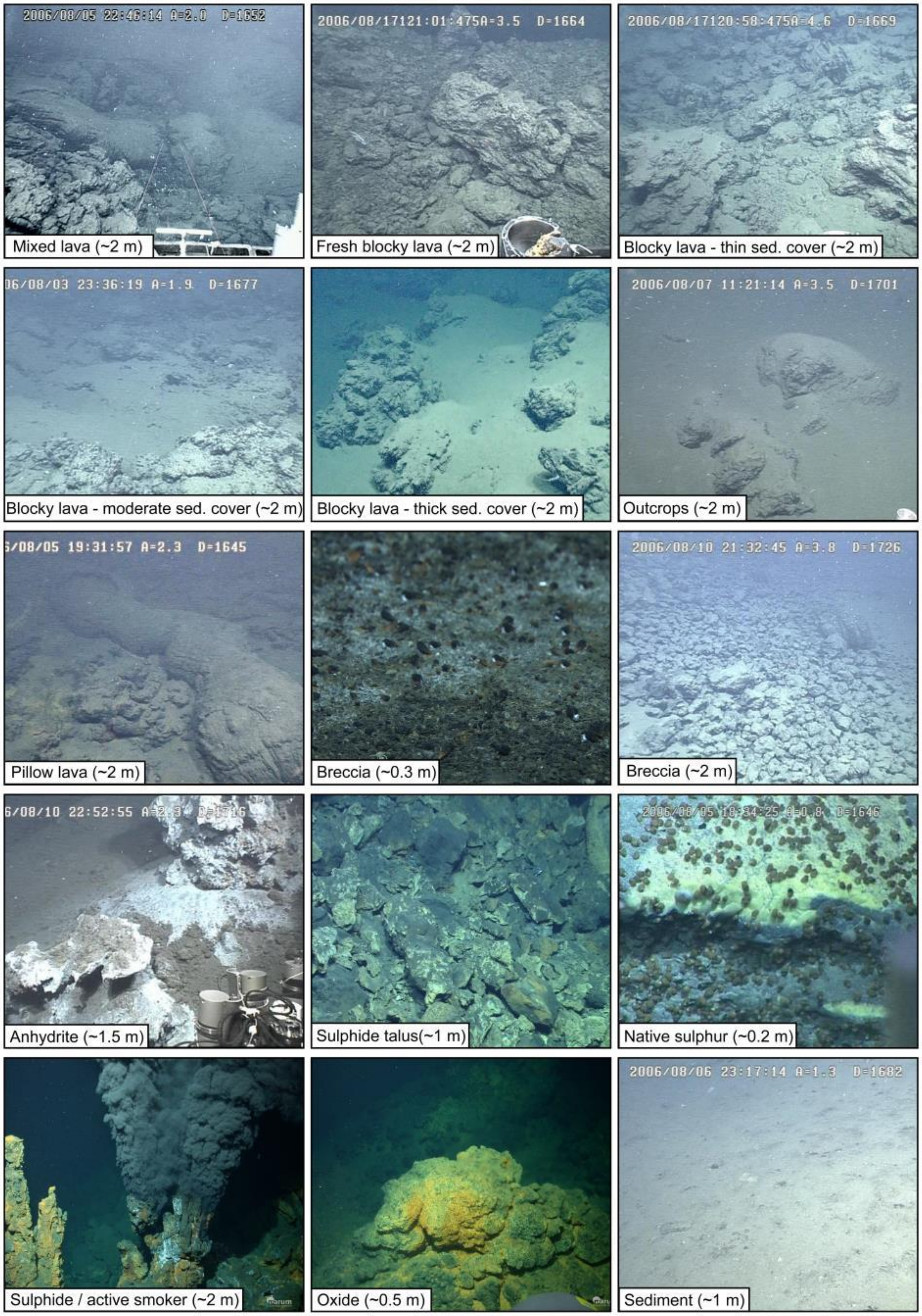

Fig. 5: Examples of the major mapping units with estimated picture width

4. Results

Detailed geological mapping was conducted in the five main hydrothermal fields of the PACManus hydrothermal area on the crest of central Pual Ridge. Following the strike of Pual Ridge from southeast to northwest, these fields are Tsukushi, Snowcap, Fenway, Satanic Mills, and Roman/Roger's Ruins (Fig. 4, supplemental video). Rock sample analyses and sample numbers are given within brackets (e.g. #1 – 72 wt.% SiO2) and their location can be found in the geologic maps (Figs. 6 – 9) and in table S1 (supplementary).

4.1 Geologic setting of vent fields

4.1.1 Tsukushi

Tsukushi (Jap. for cat-tail) is also known as Field G (Binns and Scott, 1993; Hashimoto et al., 1999). It is located at the southwestern end of the PACManus hydrothermal area at 1660 mbsl and extends about 40 m east-west (Fig. 6). Tsukushi is bordered to the north by a thick blocky lava flow that emanates from the summit of Knoll #1 (#2 – 72.5 wt.% SiO2; aphanitic, fresh lava) of Pual Ridge neovolcanic zone ~150 m to the north and terminates in a well-defined flow front a few meters from the Tsukushi vent field. The underlying lava unit hosts the hydrothermal field (#1 - 67.4 wt.% SiO2). Tsukushi is separated into two parts: the western side has active and diffuse fluid discharge and oxide deposits, while the eastern side has inactive sulphide chimneys (table 1).

The central Pual Ridge neovolcanic zone to the north of Tsukushi and west of the Snowcap (Fig. 6) is comprised of two volcanic knolls (knoll #1 & #2, Figs. 4, 6) that rise 20 - 30 m high above the surrounding seafloor. Their slopes consist of blocky lava with moderate pelagic sediment cover. The eastern knoll (knoll #2) is characterised by several meter-deep trenches floored with pillow lava that has a heavy sediment cover. Both knolls have flat tops with a thick sediment cover and occasional outcrops of lava that is often brecciated. Some areas show whitish-yellowish staining, which may be due to bacterial activity. Patches of breccia occur, but have small lateral extent.

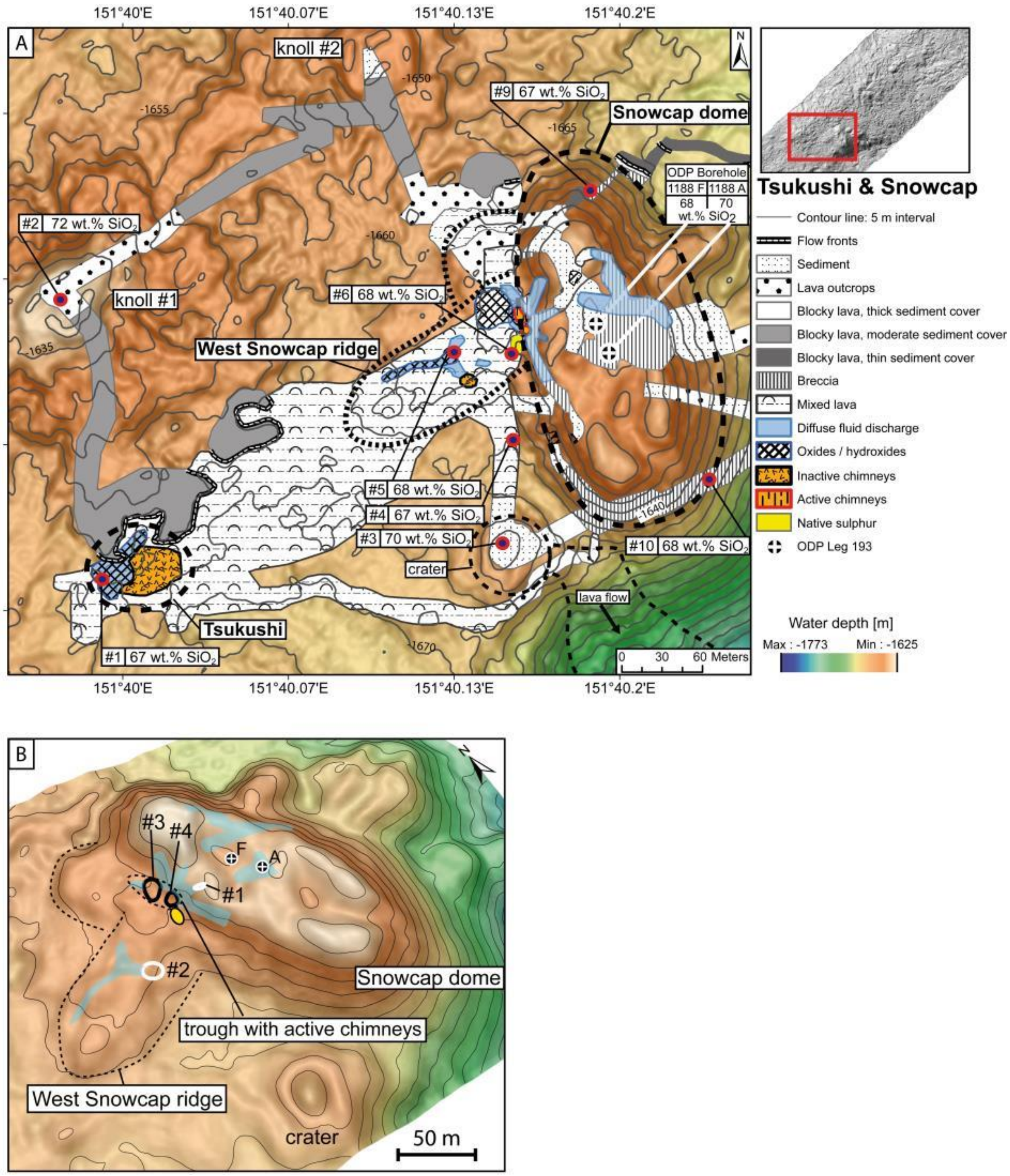

Fig. 6 a: Geological map of the southwest PACManus area. Shown are all mapped seafloor structures on the AUV bathymetry (1 m grid size) with contour lines at in interval of 5 m.

6 b: Oblique projection of the Snowcap area with prominent structures. Blue areas - diffuse venting; red dots – ODP drill sites 1188; yellow – native sulphur plates; black circles – active chimney cluster; white circles – inactive chimney cluster.

Hydrothermal field	Tsukushi West	Tsukushi East
Description	Diffuse discharge of warm fluids through cracks in the lava with small (meter-sized) patches of knobby oxide mounds (e.g. see panel "Oxides" in Fig. 5)	Two chimney clusters with diameters <10 m dominate the smoker site with columnar chimneys up to 13 m high with snow-white, cone-shaped tops.
Extent	56*32m (1792m^2)	35*35m (1225m^2)
Hydrothermal activity before 2006	No data	Active black, grey and white fluid discharge in 1996 ($T_{max.}$ 268°C; Hashimoto et al., 1999)
Hydrothermal activity in 2006	Diffuse discharge, T_{max}. 62°C	Only diffuse flow, clear fluids from chimneys' base
Hydrothermal activity in 2011	Diffuse discharge, T_{max}. 53°C	No fluid flow observed

Table 1: Description of hydrothermal discharge sites and temporal changes in the Fenway hydrothermal field.

4.1.2 Snowcap

Snowcap hydrothermal field is also known as Mont Blanc/Kai Kai site and Field D (Binns and Scott, 1993; Hashimoto et al., 1999). The Snowcap field (Fig. 6) is characterised by a prominent dome rising to about 1635 mbsl on the flank of the Pual Ridge with a largely sediment-covered summit. Moderately sedimented and apparently younger lava flows protrude from the sediment in a few places, especially in the northern part of the area. Eponymous for Snowcap is a laterally extensive area on the seafloor with a pronounced white coating, which was visible during the early photo sled surveys (Binns and Scott, 1993) and in 2006 (supplemental Fig. S2). The HD video recordings of 2011 revealed that these "white patches" are areas of diffuse venting through breccias that are densely colonised by microbial filaments along with tiny crustaceans, sea anemones, and gastropods.

Two small craters, 1-2 m deep and 3-4 m in diameter were mapped in 2006 on top of Snowcap dome. The surrounding slopes are steeply dipping (30±5°) and predominantly covered by pelagic sediment with occasional breccia fields or lava outcrops.

The West Snowcap ridge extends in a southwesterly direction from the foot of the Snowcap dome 150 m towards Tsukushi and is about 40 m wide (Fig. 6). The West Snowcap ridge (#5 – 67.7 wt.% SiO2) was apparently built by several eruptions differing in age as indicated by the variable thickness in sediment cover and lava morphology ranging from heavily sedimented lava and moderately sedimented slabby, jumbled lava to lightly sedimented chaotic jumbled lava with occasional pillow tubes. The lightly sedimented centre of the elongate ridge hosts a diffuse venting site (~700 m^2) with an inactive chimney cluster and a small crater-like depression (10 m across, 4 m deep).

A narrow, sediment-covered trough marks the intersection of the ridge with the Snowcap dome. Inside this trough, active black smoker venting occurs at chimney clusters #3 and #4 (Fig. 6b). The entire Snowcap vent field hosts four chimney clusters (Fig 6, table 2).

Decimetre thick slabs of native sulphur occur south of the Snowcap vent field and form a small mound (2 - 3 m high, ~ 13 m long; Figs. 5, 6). These slabs are colonised by many small gastropods, which – like the native sulphur – were not observed elsewhere in the PACManus hydrothermal area. Besides the sulphur slabs, pieces of woody and tube pumice were collected (#6 – 67.9 wt.% SiO2).

Sulphuric acid-rich vent fluids form such deposits, but the Snowcap vent fluids in 2006 were not sulphuric acid-type fluids (Reeves et al., 2011), indicating that the sulphur slabs must have formed during an earlier stage, when the magmatic SO2 flux was higher. Auzende et al. (1996a) observed white smoker activity at the Snowcap field in 1996. Also, abundant native sulphur as breccia cement in samples collected from the Snowcap dome indicates that discharge of SO2 must have been pervasive during this earlier stage. This is consistent with the presence of pyrophyllite-rich alteration assemblages in the drill core recovered from Snowcap (Paulick and Bach, 2006; Binns et al., 2007).

The area between Tsukushi and Snowcap is characterised by several different lava types, which often build up small (< 10 m high) mounds of jumbled lava morphology with moderate sediment cover. Pillows and mega pillows seem to be developed mainly at the foot of the mounds, whereas flattened lava lobes that are occasionally fractured, cover greater areas. Sample #4 was collected at this location with 67.2 wt.% SiO2.

Southeast of this area, a circular volcanic cone rises above the seafloor and is covered by pelagic sediment ("crater" in Fig. 6). The cone is 30 to 35 m in diameter and features a prominent crater 8 meters deep (#3 – 70.1 wt.% SiO2). A blocky lava flow originates from the crater's east slope and extends downslope to southeast (Fig. 6a).

The two ODP boreholes (1188A and 1188F) were drilled into the centre of Snowcap dome to depths of 190 and 360 mbsf respectively (Shipboard Scientific Party, 2002). While core recovery was poor (6.8-18.3%), recovered rocks indicated moderately porphyritic dacite lavas and hydrothermally altered aphyric lavas (Paulick et al., 2004) that were relatively thick and coherent based on downhole logging results (Bartetzko et al., 2003). Rock sample #8 originates from 9.8 mbsf in 1188A (#8 - 68.3 wt.% SiO2; Paulick et al., 2004). Both holes have steel re-entry cones through which no fluid discharge has been observed.

Two rock samples have been collected on the slope of Snowcap dome (#9 & #10). Sample #9 (#9 – 66.6 wt.% SiO2) is a piece of aphyric, vesicular lava with sparse plagioclase phenocrysts taken from a prominent lava flow on the northern slope. Sample #10 (#10 – 68.1 wt.% SiO2) is a piece of aphyric, vesicular lava collected as breccia from the southern slope. Rock sample #7 is a piece of aphyric, breccia from the top of Snowcap dome (#7 – 69.8 wt.% SiO2).

Hydrothermal field	**Snowcap discharge sites**			
Site	**Chimney cluster #1**	**Chimney cluster #2**	**Chimney cluster #3**	**Chimney cluster #4**
Description	Group of a few small (<1 m) chimneys	Numerous solitary, knotted, 3 - 4 m high chimneys.	Several solitary chimneys with one cluster of branched 6 - 7 m high chimneys with diffuse and rare focused fluid discharge.	Chimney complex with a diameter of ~2 m at its base. Several inactive chimneys branch towards the top.
Location	On the western slope of Snowcap dome on top of a small (~2 m wide) lava flow	On the southern slope of the central West Snowcap ridge.	Inside trough between West Snowcap Ridge and Snowcap dome	Inside trough between West Snowcap Ridge and Snowcap dome
Hydrothermal activity in 2006	No data	Inactive chimneys. Limited diffuse discharge of clear fluids through chimneys' base (T_{max} 63°C)	Several inactive chimneys with few active black smokers with T_{max} 179°C	T_{max} 151°C
Hydrothermal activity in 2011	Inactive	No data	Active black smoker / T_{max} 224	Clear fluids / T_{max} 34°C
Diffuse discharge				
The mapped area of diffuse fluid discharge at the foot of, and on top of Snowcap dome is estimated to be ~2970 m².				

Table 2: Description of hydrothermal discharge sites and temporal changes in the Snowcap hydrothermal field.

4.1.3 Fenway

The Fenway hydrothermal field is situated east of Snowcap on the southeast flank of the Pual Ridge in a depression surrounded by steep (30°) slopes to the W, NW and N (Figs. 4, 7). The vent field was discovered during the Magellan-06 cruise and sits halfway between the Satanic Mills and Snowcap vent fields. Hashimoto et al. (1999) mentioned the existence of diffuse venting at the location of Fenway but the main chimney sites of Fenway were not discovered until 2006. It is uncertain if the main focused venting complex of chimneys existed in 1996.

Fenway consists of four clusters of hydrothermal vents and a central black smoker complex (Big Papi) at a water depth of ~1715 m (table 3). Big Papi is the central mound in the Fenway hydrothermal field (Fig. 7). The base of the mound is covered exclusively with white or dark-grey sediment that is distinct from the light-grey, presumed pelagic sediment at greater distances from the structure. Prominent outcrops of massive anhydrite mark the northern border of Big Papi. These anhydrite deposits show clear signs of dissolution and emerge from dark sediment. The most vigorous fluid discharge is observed from cracks and crevices on the summit of the mound. Scattered multiple branched chimneys also occur on the northern slope of the structure. In some places strings of filigree chimneys that are only a few cm in diameter decorate fissures.

In 2006, the Big Papi mound was the most vigorous venting black smoker site of PACManus. In 2011, the discharge of black smoker fluids declined based on visual criteria. Diffuse venting is prominent in the immediate vicinity of Big Papi manifested by shimmering water streaming up from the surrounding anhydrite sand and sediment. It is noticeable that, in spite of the range in venting styles, only shrimp live on Big Papi while other members of the typical hydrothermal vent fauna are absent.

To the west and south, Big Papi is bordered by a 2 – 3 m high parapet, littered with indurated slabs of sediment. A small ridge extends to the southeast from the parapet and consists of rust-red coloured massive sulphides with volcanic and sulphidic rock fragments on its flanks. At ~1725 m, the ridge terminates in a cliff with volcanic breccia and sulphide rocks. Remnants of chimney bases with a diameter of several tens of centimetres can be seen in the breccia pile.

The slope south and southeast of Big Papi consists of an apparently young volcanic and sulphidic talus deposit, which shows little or no sediment dusting.

Two mounds with flat plateaus mark the slope west of Big Papi (Fig. 7). On the upper mound at 1680 mbsl, blocky lava with a thick sediment cover is present. On the lower mound (elevation change is 15 m) sediment thickness is thin and overlapping thin (< 10 cm thick; < 50 cm diameter) lava lobes cover the centre of the mound.

The northwestern slope of Fenway features virtually continuous sediment cover, except for one area of blocky lava, which is also heavily sedimented. The flow front of that blocky lava flow is located just 5 m north of Big Papi. At the base of the flow front, lava rock fragments form a small breccia field. A ~10 m wide entirely sedimented corridor separates the blocky lava flow from a large area of diffuse fluid discharge on the northeastern slope of the Fenway field, where a dome-like mound is present (Fenway dome). In this ~80 m wide section (diffuse dome site, Fig. 7b), diffuse hydrothermal activity is abundant with widespread patches of mussels, gastropods, tube worms, anemones, and crabs. At the foot of the Fenway dome lava outcrops become increasingly covered by sediment and breccias.

The activity in the smaller chimney clusters around Big Papi and in the diffuse dome site apparently has not changed much between 2006 and 2011.

The area on top of Fenway dome is dominated by breccia (fresh pumice clasts and angular lava fragments) that are cemented in place. This cementation is clearly visible on the edge of a plateau where, in a few places, decimetre-thick flanges of cemented breccia outcrop. A temperature of 11°C was measured several centimetres deep in the sediment at this location in 2006. Rock sample #13 (68.9 wt.% SiO2) originates from the top and sample #14 (67.7 wt.% SiO2) from the edge of Fenway dome (Fig. 4). Another rock sample was collected from the sediment covered area between Fenway dome and Big Papi with a relatively low silica content (#12 – 64.1 wt.% SiO2) whereas a sample west of Big Papi has a relatively high silica content (#11 – 70.4 wt.% SiO2).

A thinly sedimented blocky lava flow with 3 – 5 m high flow fronts is present to the north and east of Fenway dome. The lava flow is well-defined in the bathymetry due to steep flow fronts and can be traced for about 180 m downslope (Fig. 7). Just ~10 m south of this pronounced flow front and in the south-eastern corner of the “Fenway” area we found another small hydrothermal field, which we named “Mimosa”. This field is composed of two small sites with extinct chimneys with diffuse venting through trunks and underneath flanges. The Solwara 8 vent field is outside of the ABE microbathymetry basemap but features clusters of ~12 m high chimneys, about 150 m southeast of the Mimosa field (Fig. 4).

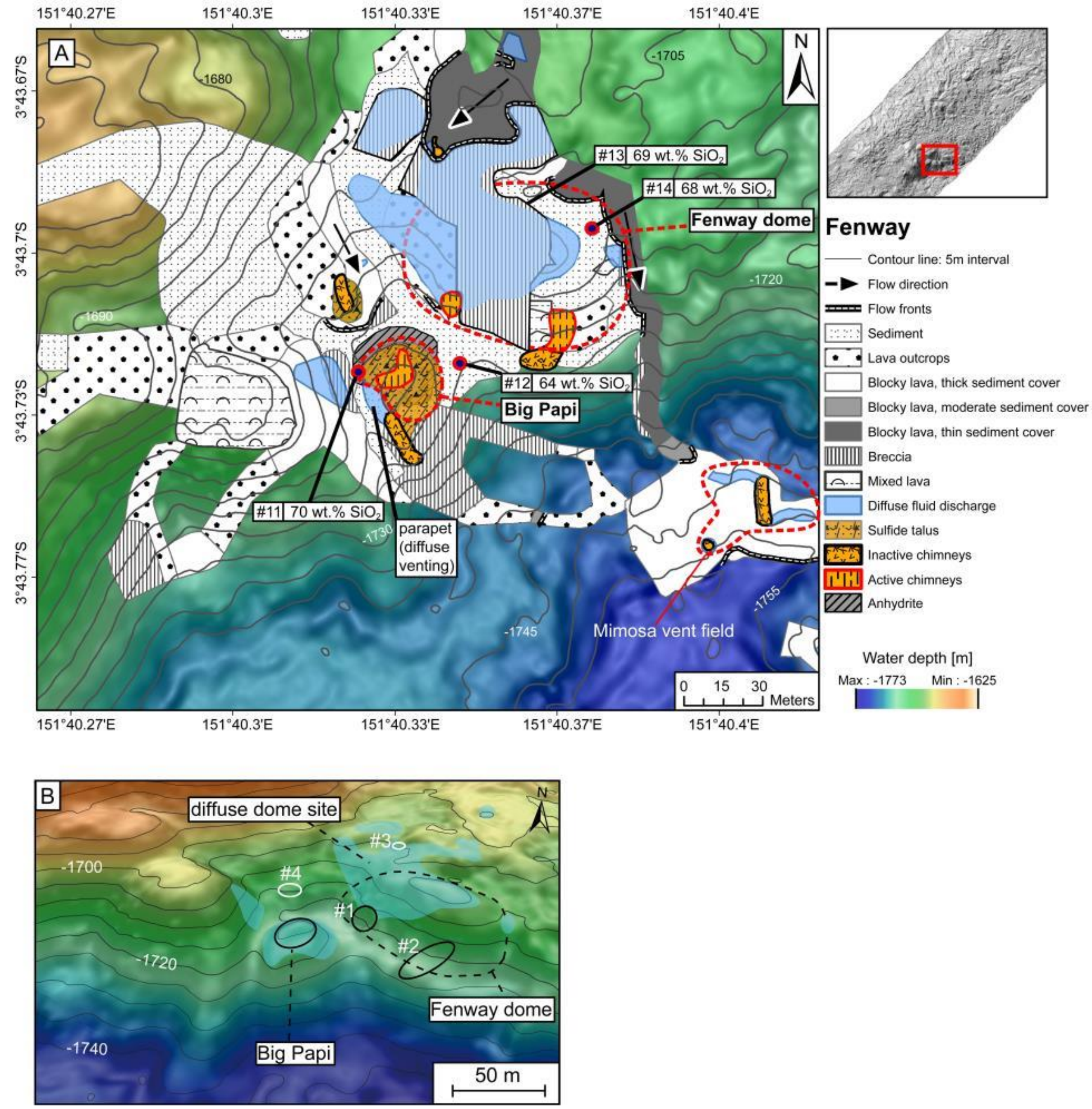

Fig. 7 a: Geologic map of the Fenway hydrothermal vent site. Shown are all mapped seafloor structures on the AUV bathymetry (1 m grid size) with contour lines at in interval of 2 m.

7 b: Oblique projection of the Fenway hydrothermal area with 5 m contours. Blue areas - diffuse venting; black circles – active chimney cluster; white circles – inactive chimney cluster.

Hydrothermal field	Fenway				
Site	Chimney cluster #1	Chimney cluster #2	Chimney cluster #3	Chimney cluster #4	Big Papi
Description	Slim (<20 cm), solitary chimneys (max. 8 m)	Cluster of solitary and branched chimneys (< 5 m).	Small cluster of a few chimneys (<2 m in height). Abundant empty gastropod shells	Several meters high columnar chimneys. Up to several tens of cm in diameter.	Mound of anhydrite and sulphide sand with active chimneys, chimney talus, massive anhydrite-sulphide blocks.
Location	~ 15 m NE of Big Papi on top of a lava flow front at the western foot of Fenway dome	at the south-western foot of Fenway dome	North of Fenway dome, chimneys grew in front and on top of blocky lava flow front.	North of Big Papi on top of a lava flow front	centre of Fenway field with surrounding parapet
Hydrothermal activity in 2006	T_{max} 330°C partly active black smoker chimneys	Mainly inactive chimneys. Clear fluids discharge from below a flange	inactive	inactive	T_{max} 358°C Most vigorous black smoker vent site of PACManus - No fluid flow through parapet
Hydrothermal activity in 2011	T_{max} 313°C Similar activity as 2006	Similar activity as 2006	inactive	inactive	T_{max} 304°C Black smoker fluid discharge decreased - Vigorous diffuse fluid discharge through parapet: T_{max} 90°C
Diffuse fluid discharge					
At the sites with diffuse fluid flow only, discharge occurs through volcaniclastic covered seafloor and around outcrops with abundant fauna. No changes were observed between 2006 and 2011. The total area with diffuse fluid discharge at the Fenway field is estimated to be ~4450 m² (incl. diffuse dome site: 3300 m²).					

Table 3: Description of hydrothermal discharge sites and temporal changes in the Fenway hydrothermal field.

4.1.4 Satanic Mills

Satanic Mills is also known as Field E, Black Smoker Site and the Juvenile Site (Binns and Scott, 1993; Hashimoto et al., 1999). It is an active hydrothermal field with numerous isolated discharge sites northeast of the Snowcap dome at 1695-1675 m (Fig. 8). Apart from a few areas, Satanic Mills is dominated by three blocky lava flow units (#1, #2, #3), which can be mapped based on their 3 – 6 m high steep flow fronts, which are apparent in the ABE microbathymetry map (Fig. 8). The oldest flow #1 is overlaid by flow #2, which itself is overlaid by the youngest flow #3.

Blocky lava flows #2 and #3 overlie sediment-covered mixed lava morphologies as can be deduced from seafloor mapping in the southwestern portion of the Satanic Mills area (Fig. 8). In that mixed underlying lava unit, well developed pillow lava tubes (#15 – 67.9 wt. % SiO2) are present and disappear towards the west under an increasing thickness of sediment.

ODP hole 1191A attempted to drill into the Satanic Mills field, but got stuck at 20 m and then the hole collapsed ending operations there (Shipboard Scientific Party, 2002a). A rock sample from 0.6 mbsf of aphyric dacite pressumably represents flow #1 (#16 – 1191A – 69 wt.% SiO2; Paulick et al., 2004). Monecke et al. (2007) analysed glassy dacite sampled from flow #2 via TV-grab on So-166 (#24 - 69.2 – 70.1 wt.% SiO2).

The majority of the hydrothermal discharge sites (table 4) are located near the front of flow #2. In areas of compact flow fronts, the sulphide chimneys have grown directly out of the contact zone between the flow front and the underlying formation. In areas where an apron of breccia decorates the flow front, the sulphide chimneys sit on top of the breccia pile in discrete clusters. These active vents emit predominantly black smoker fluids from clusters of numerous branched, thin (max. 10 cm) chimneys. Minor chimney clusters and patches of diffuse venting are also found sparsely distributed apparently unrelated to any lava flow fronts. These sites are constrained to small depressions in the lava flow. The distance between the northern and southernmost chimney clusters is ~100 m. The east-west dimension of the field is a maximum width of 40 m.

Hydrothermal field	**Satanic Mills**		
Site	**Central chimney cluster**	**Isolated clusters**	**Diffuse discharge sites**
Description	Countless chimneys (<10m high; <20cm diameter)	Several small clusters of chimneys	Patches of diffuse venting with vent fauna
Location	Centre of Satanic Mills field; along and on top of the flow front of blocky lava flow #2	Along cracks and flow fronts of lava flow #2 around the central chimney cluster	Along cracks and depressions inside lava flows #1 & #2
Hydrothermal activity in 2006	T_{max} 295°C Many active black smoker chimneys with CO_2 rich fluids (>200 mM CO_2)	Most clusters had few active chimneys	Active diffuse discharge
Hydrothermal activity in 2011	T_{max} 345°C Activity similar to 2006. Liquid CO_2 venting indicates similar CO_2 enrichment.	Less active chimneys	Similar activity as in 2006

Table 4: Description of hydrothermal discharge sites and temporal changes in the Satanic Mills hydrothermal field.

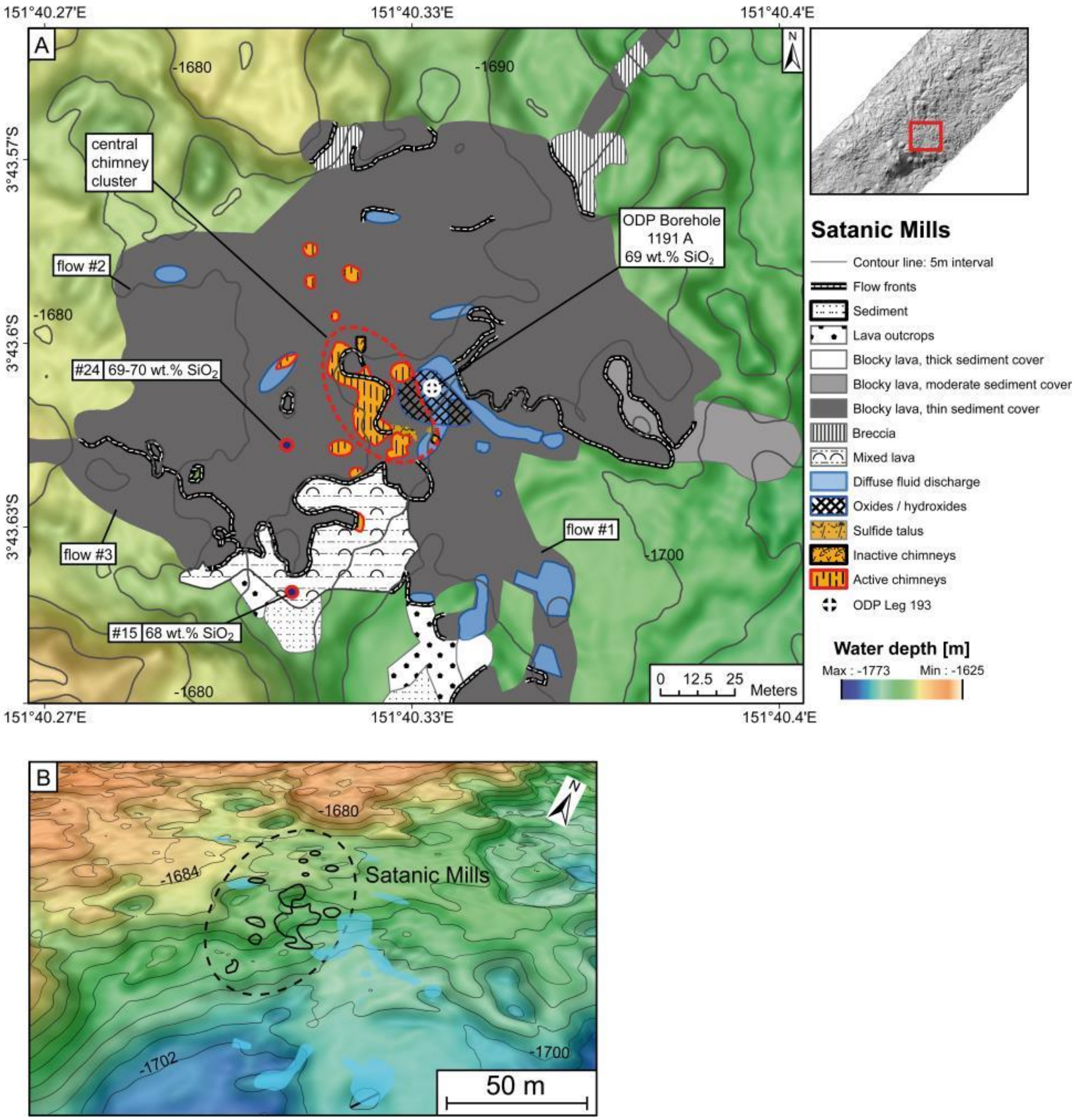

Fig. 8 a: Geologic map of Satanic Mills hydrothermal vent field. Shown are all mapped seafloor structures on the AUV bathymetry (1 m grid size) with contour lines at in interval of 5 m.

8 b: Oblique projection of the Satanic Mills hydrothermal vent field with 2 m contours. Blue areas - diffuse venting; black lines – active chimney cluster

4.1.5 North PACManus Vent Area

Roman Ruins appears to be directly on strike with the central fissure system of the neovolcanic zone. The separate but smaller Roger's Ruins vent field is located ~200 m northwest of Roman Ruins, perpendicular to this neovolcanic trend. Interestingly, further out, another 200 m along this perpendicular flow line trend is yet another vent field, Solwara 7 (Figs. 4, 9).

The prominent SW-NE striking central edifice of the neovolcanic zone (#17 – 71.3 wt.% SiO2; #18 – 71.8 wt.% SiO2) of the PACManus hydrothermal area terminates along strike to the northeast at the location of the Roman Ruins hydrothermal vent field (Figs. 4, 9). To the northeast of Roman Ruins, another separate volcanic centre begins. Thus, this hydrothermal field occurs in a small swale between the two volcanic centres along strike with the neovolcanic zone.

A blocky lava knoll with a moderate to thick sediment cover (Fig. 9) lies between Roman Ruins and Roger's Ruins and separates the two hydrothermal fields from each other. The region southeast of Roman Ruins is characterised by blocky lava flows without any evidence of hydrothermal activity. Sediment thickness increases markedly with increasing distance from Roman Ruins so that 200 m to the southeast of the vent field, the sediment cover is almost continuous with only sparse outcrops of lava (#23 - ODP 1190C - 67.8 wt.% SiO2).

4.1.5.1 Roman Ruins – Roman Ruins, also known as Field F and the Chimney Forest site (Binns and Scott, 1993; Hashimoto et al., 1999), is located at a depth of ~1675 m and is the largest hydrothermal field in the entire PACManus district. It was discovered by Binns and Scott (1993) and was revisited by Hashimoto et al. (1999) but detailed information about the fluid composition and temperature were not reported.

Roman Ruins area is characterised by small mounds, which exhibit countless chimneys (Fig. 9; table 5). The depressions between the mounds are mainly covered by piles of sulphide talus. In many places, identification of the seafloor was impossible due to limited visibility created by dense black smoke emitted by the vents.

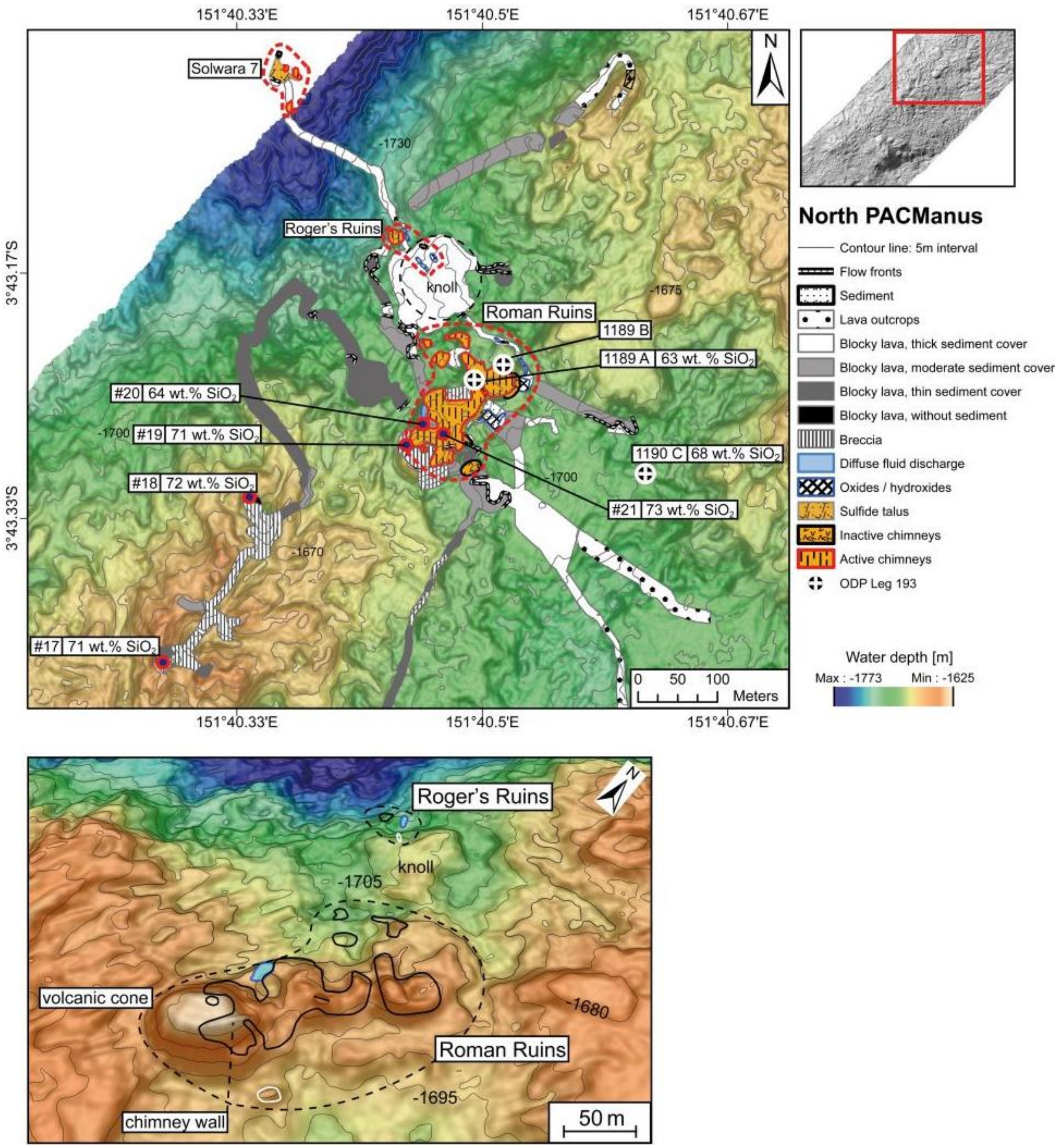

Fig. 9 a : North PACManus. Shown are all mapped seafloor structures including the two hydrothermal fields Rogers Ruins and Roman Ruins on the AUV bathymetry (1 m grid size) with contour lines at in interval of 5 m.

9 b: Oblique projection of the Roman Ruins and Rogers Ruins hydrothermal area with 5 m contours. Blue areas - diffuse venting; black lines – active chimney cluster; white circles - inactive chimney cluster.

Hydrothermal field	Roman Ruins		
Site	**Chimney sites**	**Chimney wall**	**Diffuse discharge**
Description	Clusters of chimneys 0.5 to 7 m high, columnar, solitary or highly branched with grey to black fluids. Many of the columnar chimneys are topped with white, beehive-like cones that show diffuse venting through their fragile walls.	Compact wall of coalesced chimneys issuing black smoker fluids through countless orifices. A small (< 3m wide) lava flow seems to originate from the wall's base.	In the gullies between mounds, clear fluids discharge from cm-wide cracks in the volcanic basement. Also, at the base of some mounds with chimneys, clear fluids discharge diffusely.
Location	All chimneys formed on or around little mounds or ridges.	Part of the main field; at the eastern corner of the volcanic cone.	In between mounds and around the chimney cluster.
Hydrothermal activity 2006	$T_{max.}$ 341°C	$T_{max.}$ 341°C Activity only surpassed by Big Papi	$T_{max.}$ 106°C
Hydrothermal activity 2011	$T_{max.}$ 334°C Activity at scattered chimney clusters subsided.	Similar to 2006, no temperature measurement	No data

Table 5: Description of hydrothermal discharge sites and temporal changes in the Roman Ruins hydrothermal field.

Volcanic rocks outcrop in a depression between a volcanic cone and a chimney decorated mound at the southwestern end of the Roman Ruins field. A rock sample was taken at the centre of this depression (#21 – 73.3 wt.% SiO2) and another sample 27 m apart, towards the northwestern end of the hydrothermal field (#20 – 64.4 wt.% SiO2).

The circular volcanic cone with a flat plateau and ~35° steep slopes marks the southwestern end of the Roman Ruins hydrothermal field. The northern and western slope is dominated by chimneys and sulphide talus with minor outcropping of volcanic rocks (#19 – 71.4 wt.% SiO2). In contrast, the southwestern slope shows no signs of hydrothermal activity and is dominated by variable angular, unconsolidated volcanic breccia covering the area. Sediment and breccia cover the centre of the plateau, where a solitary branched smoker has grown. At the eastern edge of the plateau, a small lava flow can be traced uphill to the base of the chimney wall.

ODP boreholes 1189A and 1189B were drilled in the northeastern half of Roman Ruins (Shipboard_Scientific_Party, 2002) to a depth of 125.8 and 206 mbsf respectively. 1189B is in an area surrounded by active chimneys. The cased hole showed no signs of hydrothermal discharge either during or after drilling. Hole 1198A could not be found during later expeditions. Although the boreholes are located only ~35 m apart, the drilled lithologies appear to vary substantially between the holes. Intensely altered aphyric dacite dominates core 1189A with fresh dacite (#22 - 1189A - 62.9 wt.% SiO2) limited to the top section (<10 mbsf) but with no significant mineralised zones. In contrast, 1189B was cased for the upper 31 m and immediately intersects a hydrothermal stockwork zone (31 - ~85 mbsf). Shallow drilling close to 1189B on Condrill cruise So-166 in 2002 revealed that the mineralised zone is also present in the shallow subsurface (Petersen et al., 2005).Variably altered dacites with sparsely local stockwork veining dominates the deeper parts of hole 1189B (Shipboard_Scientific_Party, 2002; Paulick et al., 2004).

East of 1189B, at the end of the main chimney field, no chimneys were found, but oxide deposits form a small mound with a central depression a few meters in diameter. To the northwest of 1189B, the topography is characterised by narrow (<10 m) but steep volcanic ridges with crests completely paved with active chimneys. Some of the chimneys are surrounded by oxide mounds that are not included in the map (Fig. 9) due to their small lateral extent. A small SW-NE trending trench, formed by surficial lava morphology, defines the northern edge of the Roman Ruins field. A volcanic knoll north of the trench shows thick sediment cover and a few small inactive chimneys and oxide mounds. The Roger's Ruins hydrothermal field lies at the foot of the northwestern slope of that knoll (Fig. 9).

4.1.5.2 Roger's Ruins – Roger's Ruins is located about 35 m deeper than Roman Ruins on the northern flank of Pual Ridge in 1710 m water depth (Fig. 9, table 6). Roger's Ruins is situated on a small terrace directly at the foot of a volcanic knoll. This volcanic knoll defines a ~100 m wide area without hydrothermal activity which separates Roger's Ruins from Roman Ruins. The immediate northern and western slope of Roger's Ruins is covered by sulphide and volcanic breccia.

4.1.5.3 Solwara 7 – Active hydrothermal vent site, Solwara 7, at a depth of ~1800 m is located just outside the ABE microbathymetry map area (Figs. 4, 9; table 6). The vent field lies downslope of Roger's Ruins where the seafloor is dominated by blocky lava flows covered by a thick sediment cover with a few mega pillow features that emerge at the base of lava flow lobes. Several old discharge sites closer to Solwara 7 are marked by collapsed and sediment-covered inactive chimneys.

Hydrothermal field	Roger’s Ruins		Solwara 7
Site	**Chimney site**	**Diffuse**	**Chimney site**
Description	One large and one small cluster of chimneys. The small cluster is characterised by numerous active chimneys that are highly branched. The large cluster is composed of mostly inactive, columnar chimneys (max. 9 m high) with diffuse venting through their base and oxide deposits.	Diffuse fluid discharge was observed in a small, ~8 m long zone populated with small oxide mounds.	Predominantly solitary, maximum ~12 m high chimneys. No separate area with diffuse fluid discharge was observed.
Location	On a terrace at the foot of a volcanic knoll	east of the chimney site	NE of Roger’s Ruins
Hydrothermal activity in 2006	small cluster of chimneys characterised by highly branched tubes emitting large amounts of black fluids T_{max} 320°C	No data	No data
Hydrothermal activity in 2011	Small cluster: no discernible change in activity Main cluster: focused venting declined and only diffuse venting at the base of the chimneys could be observed	No data	Vigorous fluid flow through a few solitary chimneys T_{max} of 348°C. Diffuse fluid flow at the chimneys base and through sulphide talus.

Table 6: Description of hydrothermal discharge sites and temporal changes in the Roger’s Ruins and Solwara 7 hydrothermal field.

5. Discussion

Since the discovery of PACManus in 1991 it has often been described as one of the largest marine hydrothermal active areas with metal-rich precipitates (e.g. Binns and Scott, 1993; Auzende et al., 1996; Hashimoto et al., 1999; Petersen et al., 2003; Binns et al., 2007).

Figure 10 shows a summary of the dimension and position of the mapped hydrothermal discharge sites in 2011 based on 20 ROV dives with precise navigation that allows us to update earlier estimates based on photo sled work from 1991 (Binns and Scott, 1993). The overall size of the vent fields is considerably smaller than in the original estimates (Binns and Scott, 1993). In addition, several new vent fields have been added, i.e. Fenway, Solwara 6, 7 and 8 (Table S2).

Hydrothermal activity is hosted by volcanic units as visible on the seafloor but deeper features that control fluid pathways have not been assessed so cannot be discounted.

The high-resolution ABE bathymetry maps show a striking morphology with two identifiable types of volcanic terrain: steep-sided lava flows and domes.

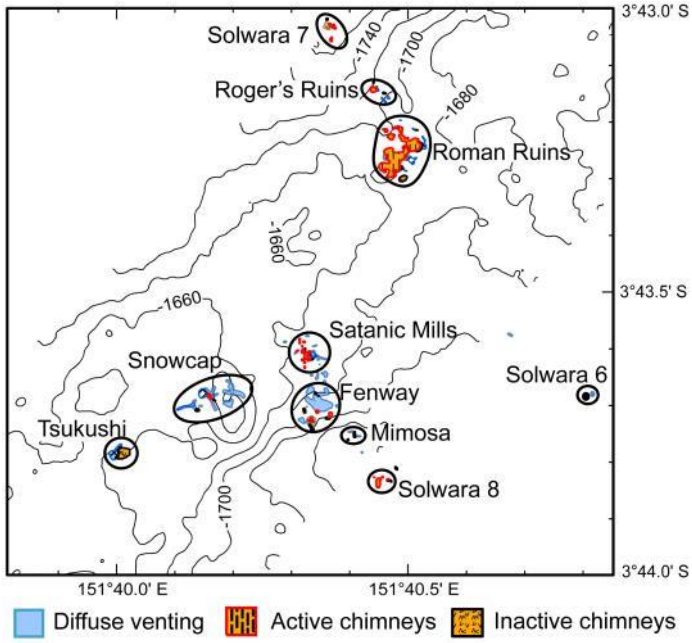

Fig. 10: Mapped hydrothermal fields in this study.

5.1. Volcanism of Pual Ridge

5.1.1 Domes

Dome-like structures are found in three locations within the PACManus hydrothermal area: Snowcap, Fenway and Roman Ruins (Figs. 3, 9). We do not distinguish between crypto-domes and domes.

Several models for subaqueous silic domes or lava lobe emplacements have been developed (e.g. Pichler, 1965; de Rosen-Spence et al., 1980; Yamagishi and Dimroth, 1985; McPhie et al., 1993; Goto and Tsuchiya, 2004). These models propose an endogenous growth with a coherent core that is surrounded by a rim of autobreccia and quench-fragmented, in situ and re-deposited, hyaloclastite. Dome growth can become exogenous when syn-eruptive injection of fresh lava into the domes or lava flows trigger lava to emerge laterally from the clastic pile and form lava lobes.

At Snowcap, ODP Leg 193 drill core had exceedingly low core recovery from the uppermost 40 m of the dome and so Bartetzko et al. (2003) used drill hole logging data to interpret Snowcap as being composed of a 35 m thick massive volcanic unit that erupted in place. Paulick et al. (2004) described the recovered rocks as fresh, moderately porphyritic dacite and interpreted this to be the most recent volcanic facies at PACManus. They also observed flow banded coherent dacite intruding into a breccia of flow banded clasts in a sample from 157.2 mbsf recovered at Snowcap indicative of endogenous growth (ODP Site 1188).

Snowcap dome is sediment covered with steeply dipping (~30°) slopes with the uppermost central part of the dome composed of unconsolidated breccia (e.g. angular fresh lava clasts, variably altered lava clasts, tube and woody pumice). Our observations corroborate the interpretation of Paulick et al. (2004), who considered the Snowcap dome to represent a dacitic volcanic unit with an brecciated outer layer and a coherent core. However, our discovery of small volume, sediment-free lava flows on top of the otherwise sedimented dome suggests that there was a more recent volcanic eruption in the Snowcap region. This eruption may be related to the extrusion of the lavas building the West Snowcap ridge, which is also largely unsedimented. Distributed around the breccia-covered dome top are patches of diffuse venting and a varied hydrothermal fauna (Fig. 6).

The second area where several dome-like structures were identified is the Fenway hydrothermal field (Fig. 7). The bathymetry shows two mounds west of Big Papi with lava flow features at their top. We assume that the flat lava lobes on the lower mound result from relatively low viscosity lava and blocky lava flow structures on the upper mound indicate lateral lava movement. We therefore interpret these structures to be constructional volcanic mounds instead of domes.

The only structure at the Fenway hydrothermal field that meets the criteria for a dome is the Fenway dome to the east of Big Papi. The Fenway dome with ~30° steep slopes features abundant unconsolidated volcanic breccia with few massive (> 1 m) glassy lava outcrops and blocks. These breccia cover the entire dome, which resembles the model of a silicic dome after McPhie et al. (1993) with a breccia rim and emerging lava lobes. Similar to Snowcap dome, there is widespread diffuse venting through volcanic breccia on Fenway dome.

The third dome-like volcanic cone (Fig. 9) is at the southwestern end of the Roman Ruins hydrothermal field and hosts the chimney wall. Unaltered, angular volcanic breccia and a small lava flow on the east slope indicate recent volcanic activity. The other slopes are either sediment covered or host active and inactive sulphide chimneys. No pumice or fine volcanic breccia compared to Fenway dome and Snowcap dome could be observed. We interpret the volcanic cone to be a constructional volcanic mound rather than a dome due to the lack of a pervasive cover of breccia, the abrupt transition between slope and horizontal plateau and the different lithology between the plateau and the slopes (fine material on the plateau vs. breccia on the slopes).

5.1.2 Lava facies in the PACManus hydrothermal area

The PACManus hydrothermal area is hosted by felsic effusive volcanic successions with little or no obvious associated tectonic activity. We have identified individual flow units and based our chronology on various characteristics that include flow morphology, sediment thickness, and chemical composition. The relatively high sedimentation rate in Manus Basin allows us to broadly distinguish different volcanic events based on the thickness of sediment cover. Sedimentation has been occurring at a rate ~15.5 cm/ka in the central Manus Basin over the past 16,000 years (Barash and Kuptsov, 1997). Hrischeva et al. (2007) calculated an even higher sedimentation rate, not corrected for compaction, of between 26.5 to 33 cm/ka for the eastern Manus Basin. In general, across the study area, the thickness of sediment cover is heavy in areas without hydrothermal activity and so identification of the underlying lithology is often impossible, despite this we can make some broad categorisations.

We define Stage-1 as the earliest phase of volcanic activity when Snowcap erupted slightly to moderately porphyritic lavas (#8, 10: 68.1 – 68.3 wt. % SiO2), forming Snowcap dome. We make the assumption that the equivalent morphology, thickness and distribution of sediment cover observed at the nearby (300 m) Fenway dome along with its similar SiO2 concentrations (#13 - 14: 67.7 - 68.9 wt. % SiO2) suggests this dome also formed during Stage-1.

The second phase of activity (Stage-2) is the intermediate stage between the heavily sediment covered domes of Stage-1 and the nearly sediment-free recent Stage-3 lavas. Stage-2 activity followed Stage-1 with the eruption of aphyric lava with slightly lower SiO2 concentrations (#1, #3 - 6, #15: 67.2 – 67.9 wt. % SiO2). This stage is characterised by hackly lava flows forming small mounds with pillowed subdomains. The sediment cover ranges from thick to moderate. The Stage-2 lavas can be found in the southwestern Satanic Mills area and on the West Snowcap ridge, as well covering the plain between Snowcap and Tsukushi (distance ~200 m). West Snowcap ridge was one of the apparent source centres during this period. Parts of this ridge stratigraphically overlie the slopes of the Snowcap dome indicating its younger age.

Dykes intruded and fed small amounts of lava (#9: 66.5 wt. % SiO2) on top of the northern part of the Snowcap dome. Although the composition differs from the other Stage-2 samples, we classify this activity at Snowcap into Stage-2 due to the proximity to the West Snowcap ridge and moderate sediment cover.

The latest phase of activity (Stage-3) erupted massive blocky lava with SiO2 concentrations between 69 and 72.5 wt. % sourced from the neovolcanic zone (Fig. 4). These flows are distinguished by their rough morphology. Several blocky flows overlap each other. The oldest flows of Stage-3 are blocky lava flows at Satanic Mills (#16, 24: 69 – 70.1 wt. % SiO2) and at knoll #1, north of Tsukushi. They have a thin to moderate sediment cover and a compacted surface with only minor breccias.

Not all of the edifices of the neovolcanic zone are formed during Stage-3 as it is assumed for the eastern part. The heavy sediment thickness in parts of knoll #1 and knoll #2 at the western neovolcanic zone indicate that parts of these knolls are remnants of eruptions ealier than Stage-1. However, a blocky lava flow (#2: 72.5 wt. % SiO2) north of Tsukushi was sourced by knoll #1 and substantiates a Stage-3 eruption at knoll #1 as this lava flow stratigraphically overly Stage-2 lava. Further, a blocky lava flow of Satanic Mills could be traced upslope towards knoll #2 affirming Stage-3 eruptions there.

Another blocky lava flow (Flow #1, Fig. 8) can be followed from Satanic Mills, south past the Fenway dome down to the lower terrace below Fenway (Figs. 6, 7) indicating relatively fluid flow behaviour compared to the lava forming the domes of Stage-1.

The youngest flows of Stage-3 are sourced from the furthest eastern edifice in the neovolcanic zone (#17, 18: 71.3 – 71.8 wt. % SiO2). The surface of these flows is dominated by breccias. Sediment thickness is thinner on these flows compared to the flows from Satanic Mills.

Based only on the chemistry, samples from Roman Ruins (#19, #21: 71.4 – 73.3 wt. % SiO2), from the crater southwest of Snowcap (#3: 70.1 wt. % SiO2) and from west of Big Papi (#11: 70.4 wt. % SiO2) maybe related to Stage-3 eruptions.

The chronologic sequence allows a classification of the major volcanic structures mapped at the PACManus hydrothermal area. But not all samples and structures could be binned into the chronologic sequence due to missing information of lava flow morphology and the obscuring thickness of sediment cover.

Sample #23 (67.8 wt. % SiO2) originates from ODP hole 1190C, E of Roman Ruins from 13.2 mbsf. It is not applicable to correlate this analysis to surficial observations and to classify this sample into the chronologic sequence.

The sediment-free tube pumices (#7: 69.8 wt. % SiO2) on top of Snowcap dome and the sediment-free spots on West Snowcap ridge (no sample) maybe signs of recent dike fed eruptions.

Three samples with less evolved compositions at Roman Ruins and near Big Papi also do not appear to be part of this chronologic sequence. The breccia sample west of Big Papi (#12: 64.1 wt. % SiO2, Fig. 7a) could have originated from the nearby Fenway dacite dome. At Roman Ruins, lavas with similar compositions (#20, 22: 62.8 – 64.4 wt.% SiO2) might be associated with the eruption of the Fenway lava lobe. There is a sharp contact between these lower Si lavas and the overlying siliceous blocky lava.

There is a possible correlation between the SiO2 content and lava morphologies at PACManus. The most rugged blocky lava flows are the most siliceous composition as might be expected from the increased viscosity. But the differences in SiO2 concentrations are too small to assign these variations solely to the effect of SiO2 on viscosity. Besides lava composition, other factors, such as the pre-flow morphology, the eruption rate, or temperature can affect lava flow type (Bonatti and Harrison, 1988; Gregg and Fink, 1995). It is therefore difficult to establish simple cause-effect relations to account for the different flow types at PACManus. Our observations do show a possible correlation between the SiO2 content and lava morphologies. It is likely that magma plumbing dynamics, including recharge and replenishment events caused fluctuations in temperature and eruption rate that led to the varied flow morphologies and rock types.

A striking feature of the Stage-2 volcanic eruptions are the abundance of dacitic pillows and flattened lava lobes, typical for low-viscosity basaltic lavas. Siliceous low-viscosity lava flows with this morphology have been observed in numerous Archean and Phanerozoic sequences and have been interpreted to result from high temperatures and high water contents (Bevins and Roach, 1979; de Rosen-Spence et al., 1980; Cas, 1992; Gibson et al., 1999; Dinel et al., 2008).

Binns (2004) found basaltic xenoliths within altered dacitic basement from PACManus. We speculate that these xenoliths may represent parental basaltic magma, which intruded into a fractionating dacitic magma reservoir. The resulting superheated low-viscosity dacitic magma could explain the observed Stage-2 lava flow morphologies.

Bartetzko et al. (2003) and Paulick et al. (2004) interpret the different lava facies from drilling at Snowcap and Roman Ruins to result from the spatial distance from the volcanic centre, with Snowcap representing a facies proximal to the main volcanic vent. This proximal facies is dominated by coherent lava with related breccia. Eruptions formed a several hundred metre thick succession of domes, syn-volcanic intrusions and lava flows (Paulick et al., 2004). Roman Ruins represented a medial facies due to the abundance of transported brecciated lava. However, our seafloor observations and mapping reveals that these drill locations have a similar distance from the PACManus neovolcanic zone (e.g. 250 – 320 m). Snowcap, Fenway and Roman Ruins all host recently active volcanic vents and no re-deposited breccia was observed at PACManus.

We conclude, based on the results of seafloor mapping, that the domes and flows represent different eruptive events sourced from different volcanic vents, distributed throughout the PACManus hydrothermal area.

5.2 Controls on the distribution and type of hydrothermal venting

The locations of most hydrothermal fields and distribution of chimneys in the PACManus hydrothermal area appear to be related to the volcanics (Fig. 11). The Tsukushi field is situated adjacent to a blocky lava flow front. Snowcap's active chimney cluster (Fig. 6b) lies at the contact zone between the western base of Snowcap dome and the West Snowcap ridge. Flow structures and morphology of the West Snowcap ridge lavas imply that the chimneys grew on top or close to the eruption centre. At Satanic Mills, most sulphide chimneys occur along the flow front of a blocky lava flow, except for one small site that is found in a collapse pit within the flow.

At Fenway, three chimney clusters surrounding Big Papi are distributed on flow fronts or volcanic outcrops. The Big Papi mound probably developed directly on top of a feeder dyke, which produced the fresh lava breccia that covers the slope below Big Papi. The small chimney site (#3, Fig. 7b) north of Fenway dome sits at a flow front of a blocky lava flow.

At Roman Ruins, most chimneys occur on small mounds (< 5 m) and ridges with some exposing volcanic outcrops at their base. This smoker field – the largest within PACManus - developed at the contact between older, relatively silica-poor (63 - 64 wt. % SiO_2) lavas and a younger constructional volcanic mound with rhyolitic lavas.

Binns et al. (2007) proposed that fluid flow at PACManus is governed by fractures rather than permeability of the host volcanic facies. However, no major fractures or faults were observed on the seafloor in the 20 ROV dives in the PACManus hydrothermal area or in the ABE microbathymetry. Instead, our results suggest that the hydrothermal discharge in the shallow subseafloor, at least at the surface, is controlled by the volcanic facies architecture and not faults or fracturing. The lava flows and domes have compact, impermeable cores with in-situ brecciated rims surrounded by re-deposited, volcaniclastic breccia (Bartetzko et al., 2003; Paulick et al., 2004). In the absence of tectonic faults and fissuring, buoyancy forces the fluids to migrate through the breccias around the compact cores to reach the seafloor. This type of volcanic permeability control appears to govern hydrothermal discharge at Tsukushi, Satanic Mills, Roger's Ruins and Fenway (except Big Papi). We speculate that hydrothermal fluids likely pool underneath the coherent cores of thick flows and domes and undergo cooling prior to reaching the surface. Chimneys grow in places where channelized up-flow from such reservoirs is favoured, e.g. along attached lava lobes (Fig. 11, Fenway). Without channelized flow, the fluids pass through the thick layer of breccia covering the domes, undergo further cooling and disperse laterally to discharge as diffuse venting fields as found at Snowcap dome and Fenway dome (Fig. 11).

Other hydrothermal discharge sites at PACManus (Big Papi, Roman Ruins) appear to be related to small volume lava lobes that sit on or near their vents and are presumably underlain by feeder dykes. Big Papi and Roman Ruins are the two hottest and most vigorous venting sites at PACManus. The emplacement of feeder dykes may cause a different type of hydrothermal venting, which reflects a shallow but transient heat source (Stoffers et al., 2006). Several features occurring with dyke propagation can enhance fluid flow along their bodies such as: micro-fracturing, cooling and contraction as well as glassy rims that get easily altered.

The complex and diverse construction of the volcanic facies architecture of Pual ridge can explain the varying hydrothermal fluid chemistry (Reeves et al., 2011) even within a few hundred meters of lateral distance.

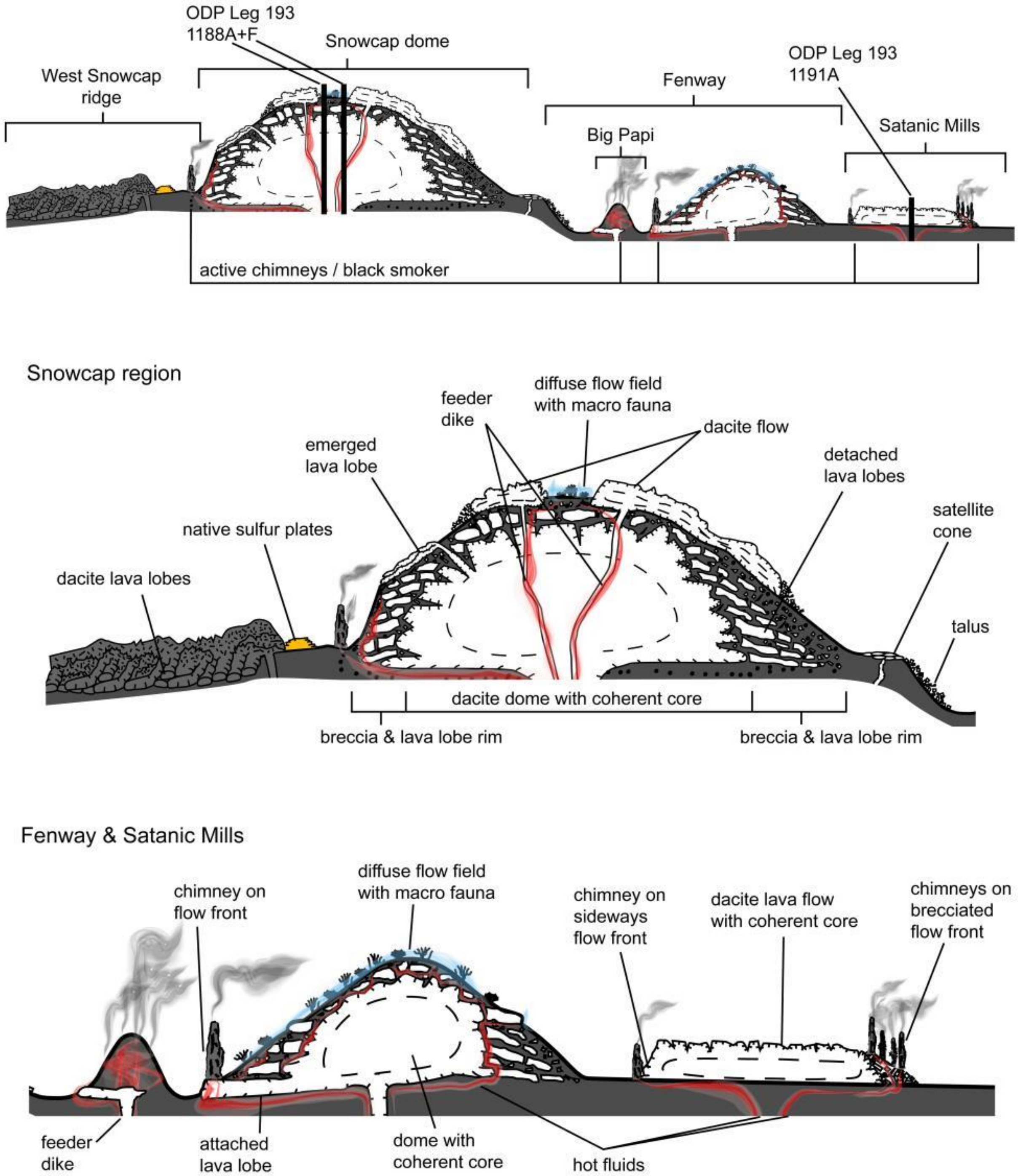

Figure 11: Sketch of the volcanic structures at PACManus with suggested fluid pathways. Not for scale.

6. Conclusions

High-resolution microbathymetry maps with meter-scale precision obtained by AUV ABE were combined with ROV video observations from the Magellan-06 and So-216 research cruises to identify landmarks in the pronounced morphology of the PACManus hydrothermal area and correct navigation offsets in seafloor features from previous expeditions to compile an internally consistent framework of observations. Accurate navigation and a quantitative GIS-based analysis revealed a smaller spatial extent of hydrothermal active areas compared with earlier estimates.

The volcanic facies show a wide range of different lava morphologies including pillows, flattened lava lobes to chaotic jumbled lava flows, massive blocky lava flows and domes. We conclude that these volcanic facies represent different stages of magmatism. In Stage-1, slightly to moderately porphyritic lavas (68 - 69.8 wt. % SiO_2) built up domes or cryptodomes. In Stage-2, aphyric lava with slightly lower SiO_2 concentrations (67.2 – 67.9 wt. % SiO_2) formed flattened lava lobes, jumbled and pillowed lava flows. In the most recent Stage-3 phase, massive blocky lava with 69 and 72.5 wt. % SiO_2 were emplaced on the seafloor constructing a volcanic ridge identified as the neovolcanic zone of the PACManus hydrothermal area.

ROV observations and AUV microbathymetry clearly document that volcanic processes dominate over tectonic processes at Pual Ridge. Hydrothermal discharge in the shallow subseafloor at PACManus appears to be controlled by volcanic structures that include domes, dykes and lava flows rather than being governed by tectonic faults and fractures. We recognise two types of volcanic permeability driven hydrothermal circulation: 1) permeability controlled fluid flow through breccias associated with domes and 2) channelized fluid flow along dikes and lava lobes.

Finally, our study demonstrates the value of combined high-resolution geophysical mapping with on bottom ROV observations and accurate navigational control within a Geographical Informational System database to resolve the detailed geological setting of the vent sites of the PACManus hydrothermal area. In particular, the autonomous underwater vehicle ABE collected detailed microbathymetry maps that formed a critical template for subsequent ROV dives and bottom exploration and sampling and sets the stage for all future such studies.

Appendix

A1: Technical specification of seafloor operations

The high-resolution bathymetry basemap used in this analysis (Fig. 4) was generated from near-bottom multibeam data collected by the AUV ABE. ABE carried a 200 kHz Simrad multibeam sonar along with a 3-axis fluxgate magnetometer, an Eh sensor (provided by Koichi Nakamura of AIST, Japan), an optical backscatter sensor and a CTD for plume sensing. ABE typically operated at an altitude of 50 m with a line spacing of 50 m providing 100% sonar coverage. The vehicle operated within a long baseline (LBL) transponder network and produced navigation tracks with <10 m resolution. The raw sonar pings were corrected for the attitude of the vehicle (pitch, roll, and heading), and merged with the navigation and interpolated onto a 1-meter grid cell map. ROV Jason-2 also operated within the LBL transponder network and supplemented these ABE data with a high-data rate (1 Hz) Doppler Velocity Log (DVL) estimate of position. Again, the accuracy of the ROV position is <10 m. During cruise SO-216, the Ultra Short-Baseline Posidonia positioning system with accuracy of < 10 m was used to navigate the ROV MARUM Quest.

The ROV Jason-2 carried three video cameras; one fixed brow camera and two pan and tilt cameras; a pilot camera and a science camera. ROV MARUM Quest carried a similar configuration, but with an HD science camera. In generating geological maps, footage from these three cameras was used to provide different perspectives of seafloor structures. The HD-camera on ROV MARUM Quest markedly improved the mapping abilities with the video data. The size of recorded objects was determined by using a laser scale device mounted on the ROV, which allowed for dimensional measurement of seafloor features.

Acknowledgement

We like to thank Sharon Allen and Thomas Monecke for detailed and thoughtful reviews which substantially improved this manuscript.

We thank the captains and crews of RV Sonne and RV Melville, the ROV teams of Jason-2 and MARUM Quest 4000, the AUV-ABE technical team and the members of the Science Parties for both cruises. Crucial help with bathymetry data processing was provided by Christian dos Santos Ferreira and Paul Wintersteller. The RV Melville work was funded by a combination of the US National Science Foundation grant OCE-0327448 and a collaborative research funding grant from Nautilus Minerals for the ABE surveys. The RV Sonne research cruise was funded through the BMBF (Grant G03216a). Additional funding, including salary support for JT, was provided by the German DFG Research Centre/Excellence Cluster "The Ocean in the Earth System". WB acknowledges support from DFG research grant BA1605/4-1.
Finally, we thank Jim Robins and Pat Pepena from Papua New Guinea (PNG) for their help with PNG research permitting.

References

Auzende, J.-M., Urabe, T., Ruellan, E., Chabroux, D., Charlou, J.-L., Gena, K., Gamo, T., Henry, K., Matsubayashi, O., Matsumoto, T., Naka, J., Nagaya, Y., Okamura, K., 1996. "Shinkai 6500" Dives in the Manus Basin : New STARMER Japanese-French Program. JAMSTEC Journal of Deep Sea Research 12, 323–334.

Bach, W., Cruise Participants, 2011. Report and preliminary results of RV SONNE Cruise SO-216, Townsville (Australia) - Makassar (Indonesia), June 14 – July 23, 2011. BAMBUS, Back-Arc Manus Basin Underwater Solfataras. Berichte, Fachbereich Geowissenschaften, Universität Bremen 280, 87.

Bach, W., Jöns, N., Thal, J., Breuer, C., Shu, L., Dubilier, N., Borowski, C., Meyerdierks, A., Pjevac, P., Brunner, B., Müller, I., Petersen, S., Hourdez, S., Schaen, A., Koloa, K., Jonda, L., MARUM Quest 4000m team, 2012. Interactions between fluids, minerals, and organisms in sulfur-dominated hydrothermal vents in the eastern Manus Basin, Papua New Guinea – A report from RV Sonne Cruise 216. InterRidge News 21, 31–34.

Barash, M.S., Kuptsov, V.M., 1997. Late Quaternary palaeoceanography of the western Woodlark Basin (Solomon Sea) and Manus Basin (Bismarck Sea), Papua New Guinea, from planktic foraminifera and radiocarbon dating. Marine Geology 142, 171–187.

Bartetzko, A., Paulick, H., Iturrino, G., Arnold, J., 2003. Facies reconstruction of a hydrothermally altered dacite extrusive sequence: Evidence from geophysical downhole logging data (ODP Leg 193). Geochemistry Geophysics Geosystems 4, 1087.

Bevins, R.E., Roach, R.A., 1979. Pillow lava and isolated-pillow breccia of rhyodacitic composition from the Fishguard Volcanic Group, Lower Ordovician, SW Wales, United Kingdom. The Journal of Geology 87, 193–201.

Binns, R., Scott, S., 1993. Actively forming polymetallic sulfide deposits associated with felsic volcanic rocks in the eastern Manus back-arc basin, Papua New Guinea. Economic geology 88, 2226–2236.

Binns, R.A., 2004. Data report: spinifex-textured basalt xenoliths at PACMANUS, Papua New Guinea, in: Barriga, F.J.A.S., Binns, R.A., Miller, D.J., Herzig, P.M. (Eds.), Proceedings of the Ocean Drilling Program, Scientific Results. College Station, TX (Ocean Drilling Program), pp. 1–19.

Binns, R.A., Barriga, F.J.A.S., Miller, D.J., 2007. Leg 193 synthesis: Anatomy of an active felsic-hosted hydrothermal system, eastern Manus Basin, Papua New Guinea, in: Barriga, F.J.A.S., Binns, R.A., Miller, D.J., Herzig, P.M. (Eds.), Proceedings of the Ocean Drilling Program, Scientific Results. College Station, TX (Ocean Drilling Program), pp. 1–71.

Bird, P., 2003. An updated digital model of plate boundaries. Geochemistry, Geophysics, Geosystems 4, 1–52.

Bonatti, E., Harrison, C.G. a., 1988. Eruption styles of basalt in oceanic spreading ridges and seamounts: Effect of magma temperature and viscosity. Journal of Geophysical Research 93, 2967.

Butterfield, D. a., Nakamura, K. -i., Takano, B., Lilley, M.D., Lupton, J.E., Resing, J. a., Roe, K.K., 2011. High SO2 flux, sulfur accumulation, and gas fractionation at an erupting submarine volcano. Geology 39, 803–806.

Cas, R., 1992. Submarine volcanism; eruption styles, products, and relevance to understanding the host-rock successions to volcanic-hosted massive sulfide deposits. Economic Geology 87, 511–541.

Craddock, P.R., Bach, W., 2010. Insights to magmatic–hydrothermal processes in the Manus back-arc basin as recorded by anhydrite. Geochimica et Cosmochimica Acta 74, 5514–5536.

De Rosen-Spence, A.F., Provost, G., Dimroth, E., Gochnauer, K., Owen, V., 1980. Archean subaqueous felsic flows, Rouyn-Noranda, Quebec, Canada, and their Quarternary equivalents. Precambrian Research 12, 43–77.

DeRita, D., Giordano, G., Cecili, A., 2001. A model for submarine rhyolite dome growth: Ponza Island (central Italy). Journal of Volcanology and Geothermal Research 107, 221–239.

Dinel, E., Saumur, B.M., Fowler, A.D., 2008. Spherulitic Aphyric Pillow-Lobe Metatholeiitic Dacite Lava of the Timmins Area, Ontario, Canada: A New Archean Facies Formed from Superheated Melts. Economic Geology 103, 1365–1378.

Edmond, J.M., Measures, C., McDuff, R.E., Chan, L.H., Collier, R., Grant, B., Gordon, L.I., Corliss, J.B., 1979. Ridge crest hydrothermal activity and the balances of the major and minor elements in the ocean: The Galapagos data. Earth and Planetary Science Letters 46, 1–18.

Gamo, T., Okamura, K., Charlou, J., Urabe, T., Auzende, J., Ishibashi, J., Shitashima, K., Chiba, H., Shipboard Scientific Party of the ManusFlux Cruise, 1997. Acidic and sulfate-rich hydrothermal fluids from the Manus back-arc basin, Papua New Guinea. Geology 25, 139–142.

Gena, K., Mizuta, T., Ishiyama, D., Urabe, T., 2001. Acid-sulphate Type Alteration and Mineralization in the Desmos Caldera, Manus Back-arc Basin, Papua New Guinea. Resource Geology 51, 31–44.

German, C.R., Lin, J., Parson, L.M., 2004. Mid-Ocean Ridges: Hydrothermal Interactions Between the Lithosphere and Oceans. American Geophysical Union, Washington, D. C.

Gibson, H.L., Morton, R.L., Hudak, G.J., 1999. Submarine volcanic processes, deposits, and environments favourable for the location of volcanic-associated massive sulfide deposits, in: Barrie, C.T., Hannington, M.D. (Eds.), Volcanic-Associated Massive Sulfide Deposits:

Processes and Examples in Modern and Ancient Settings. Reviews in Economic Geology 8, pp. 13–51.

Goto, Y., Tsuchiya, N., 2004. Morphology and growth style of a Miocene submarine dacite lava dome at Atsumi, northeast Japan. Journal of Volcanology and Geothermal Research 134, 255–275.

Gregg, T.K.P., Fink, J.H., 1995. Quantification of submarine lava-flow morphology through analog experiments 23–27.

Griffiths, R.W., Fink, J.H., 1992. Solidification and morphology of submarine lavas: a dependence on extrusion rate. Journal of Geophysical Research 97, 19,729–19,737.

Griffiths, R.W., Fink, J.H., 1997. Solidifying Bingham extrusions: a model for the growth of silicic lava domes. Journal of Fluid Mechanics 347, 13–36.

Hannington, M., Jamieson, J., Monecke, T., Petersen, S., Beaulieu, S., 2011. The abundance of seafloor massive sulfide deposits. Geology 39, 1155–1158.

Hannington, M.D., de Ronde, C.E.J., Petersen, S., 2005. Sea-Floor Tectonics and Submarine Hydrothermal Systems. Economic Geology 100th Anni, 111–141.

Hashimoto, J., Ohta, S., Fiala-Médioni, A., Auzende, J., 1999. Hydrothermal vent communities in the Manus Basin, Papua New Guinea: Results of the BIOACCESS cruises' 96 and'98. InterRidge News 8 (2), 12–18.

Herzig, P.M., 1999. Economic potential of sea-floor massive sulphide deposits: ancient and modern. Philosophical Transactions of the Royal Society A: Mathematical, Physical and Engineering Sciences 357, 861–875.

Hrischeva, E., Scott, S., Weston, R., 2007. Metalliferous sediments associated with presently forming volcanogenic massive sulfides: the SuSu Knolls hydrothermal field, eastern Manus Basin, Papua New. Economic Geologyeology 102, 55–73.

Iizasa, K., 1999. Potential Marine Mineral Resources by Hydrothermal Activity. Chemical Industry 50, 379–384.

Lee, S., Ruellan, E., 2006. Tectonic and magmatic evolution of the Bismarck Sea, Papua New Guinea: Review and new synthesis, in: Christie, D.M., Fisher, C.R., Lee, S.-M., Givens, S. (Eds.), Back-Arc Spreading Systems: Geological, Biological, Chemical, and Physical Interactions. Washington, D. C., pp. 263–286.

Martinez, F., Taylor, B., 1996. Backarc spreading, rifting, and microplate rotation, between transform faults in the Manus Basin. Marine Geophysical Research 18, 203–224.

Mcphie, J., Doyle, M., Allen, R., 1993. Volcanic textures: a guide to the interpretation of textures in volcanic rocks. Centre for Ore Deposit and Exploration Studies - University of Tasmania.

Mosier, D.L., Berger, V.I., Singer, D.A., 2009. Volcanogenic massive sulfide deposits of the world; database and grade and tonnage models, U.S. Geological Survey Open-File Report.

Park, S.-H., Lee, S.-M., Kamenov, G.D., Kwon, S.-T., Lee, K.-Y., 2009. Tracing the origin of subduction components beneath the South East rift in the Manus Basin, Papua New Guinea. Chemical Geology 269, 339–349.

Paulick, H., Bach, W., 2006. Phyllosilicate alteration mineral assemblages in the active subsea-floor Pacmanus hydrothermal system, Papua New Guinea, ODP Leg 193. Economic Geology 101, 633–650.

Paulick, H., Vanko, D.., Yeats, C.., 2004. Drill core-based facies reconstruction of a deep-marine felsic volcano hosting an active hydrothermal system (Pual Ridge, Papau New Guinea, ODP Leg 193). Journal of Volcanology and Geothermal Research 130, 31–50.

Petersen, S., Herzig, P., Hannington, M.D., Gemmell, J.B., 2003. Gold-rich massive sulfides from the interior of the felsic-hosted PACMANUS massive sulfide deposit, Eastern Manus Basin (PNG). Mineral Exploration and Sustainable Development 171–174.

Pichler, H., 1965. Acid hyaloclastites. Bulletin Volcanologique 28, 293–310.

Reeves, E.P., Seewald, J.S., Saccocia, P., Bach, W., Craddock, P.R., Shanks, W.C., Sylva, S.P., Walsh, E., Pichler, T., Rosner, M., 2011. Geochemistry of hydrothermal fluids from the PACMANUS, Northeast Pual and Vienna Woods hydrothermal fields, Manus Basin, Papua New Guinea. Geochimica et Cosmochimica Acta 75, 1088–1123.

Sangster, D.F., 1980. Quantitative characteristics of volcanogenic massive sulphide deposits. Bulletin of the Canadian Institute of Mining and Metallurgy 73, 74–81.

Sclater, J.G., Parsons, B., 1981. Oceans and continents: similarities and differences in the mechanisms of heat loss. Journal of Geophysical Research 86, 11535–11552.

Shipboard Scientific Party, 2002a. Leg 193 summary, in: Barriga, F.J.A.S., Binns, R.A., Miller, D.J., Herzig, P.M. (Eds.), Proceedings of the Ocean Drilling Program, Initial Reports. College Station, TX (Ocean Drilling Program), pp. 1–84.

Shipboard Scientific Party, 2002b. Site 1188, in: Binns, R.A., Barriga, F.J.A.S., Miller, D.J., Al., E. (Eds.), Proceedings of the Ocean Drilling Program, Initial Reports. College Station, TX (Ocean Drilling Program), pp. 1–305.

Shipboard Scientific Party, 2002c. Site 1189, in: Binns, R.A., Barriga, F.J.A.S., Miller, D.J., Al., E. (Eds.), Proceedings of the Ocean Drilling Program, Initial Reports. College Station, TX (Ocean Drilling Program), pp. 1–259.

Stoffers, P., Worthington, T.J., Schwarz-Schampera, U., Hannington, M.D., Massoth, G.J., Hekinian, R., Schmidt, M., Lundsten, L.J., Evans, L.J., Vaiomo'unga, R., Kerby, T., 2006.

Submarine volcanoes and high-temperature hydrothermal venting on the Tonga arc, southwest Pacific. Geology 34, 453–456.

Taylor, B., 1979. Bismarck Sea: Evolution of a back-arc basin. Geology 7, 171–174.

Taylor, B., Crook, K., Sinton, J., 1994. Extensional transform zones and oblique spreading centers. Journal of geophysical research 99, 19,707–19,718.

Tivey, M., Bach, W., Seewald, J., Tivey, M.K., Vanko, D.A., Shipboard Science Party, 2006. Cruise Report for R/V Melville Cruise MGLN06MV—Hydrothermal Systems in the Eastern Manus Basin: Fluid Chemistry and Magnetic Structure as Guides to Subseafloor Processes.

Van Dover, C.L., Biscotto, M., Gebruk, A., Hashimoto, J., Tunnicliffe, V., Tyler, P., Desbruyeres, D., 2006. Milestones in the discovery of hydrothermal-vent faunas, in: Desbruyeres, D., Segonzac, M., Bright, M. (Eds.), Handbook of Deep-Sea Hydrothermal Vent Fauna. Denisia, pp. 13–25.

Yamagishi, H., Dimroth, E., 1985. A comparison of Miocene and Archean rhyolite hyaloclastites: evidence for a hot and fluid rhyolite lava. Journal of volcanology and geothermal research 23, 337–355.

Supplementary

	Sample	Lat	Lon	Location	SiO_2 (wt. %)	$K_2O + Na_2O$ (wt. %)
1[1]	J2-211-2-R2	-3.72978	151.66654	Tsukushi	67.4	6.2
2[1]	J2-211-3-R1	-3.72793	151.66625	Neovolcanic zone	72.5	6.8
3[1]	J2-214-8-R1	-3.72957	151.66920	Crater (Snowcap)	70.1	6.6
4[1]	J2-214-9-R1	-3.72886	151.66928	S of W-Snowcap ridge	67.2	6.3
5[1]	J2-211-8-R1	-3.72830	151.66889	W-Snowcap ridge	67.7	6.2
6	SO-216-43-rov-11	-3.72824	151.66931	W-Snowcap ridge	67.9	6.2
7	J2-210-3-r1	-3.72828	151.66990	Snowcap	69.8	7.0
8[2]	ODP 1188A	-3.72827	151.66993	Snowcap	68.3	6.6
9	SO-216-43-rov-10	-3.7272	151.66980	Snowcap	66.6	6.4
10[1]	J2-214-7-R1	-3.72910	151.67062	Snowcap	68.1	6.6
11	J2-212-8-R1	-3.72876	151.67211	Fenway	70.4	6.4
12[1]	J2-216-11-R1	-3.72870	151.67243	Fenway	64.1	6.0
13	J2-210-6-R1	-3.72819	151.67262	Fenway dome	68.9	6.7
14	SO-216-041-rov-1	-3.72825	151.67292	Fenway dome	67.7	6.9
15[1]	J2-209-9-R1	-3.72744	151.67188	Satanic Mills	67.9	6.3
16[2]	ODP 1191A	-3.72680	151.67228	Satanic Mills	69.0	6.6
17[1]	J2-222-12-R1	-3.72385	151.67137	Neovolcanic zone	71.3	6.8
18[1]	J2-222-11-R1	-3.72201	151.67238	Neovolcanic zone	71.8	6.6
19[1]	J2-208-5-R1	-3.72142	151.67412	Roman Ruins	71.4	6.7
20[1]	J2-213-4-R1	-3.72117	151.67434	Roman Ruins	64.4	5.9
21[1]	J2-222-9-R2	-3.72126	151.67457	Roman Ruins	73.3	6.8
22[2]	ODP 1189A	-3.72072	151.67487	Roman Ruins	62.8	5.8
23[2]	ODP 1190C	-3.72172	151.67683	SE of Roman Ruins	67.8	6.7
24[3]	SO-166-58GTV	-3.727	151.67183	Satanic Mills	69.2-70.1	6.57-6.61

Table S1:

Rock samples used in this publication.

(W-Snowcap ridge= West Snowcap ridge)

*1. Analyses by Niedermeyer et al. (unpublished)

*2. Analyses by Paulick et al. (2004)

*3. Analyses by Monecke et al. (2007)

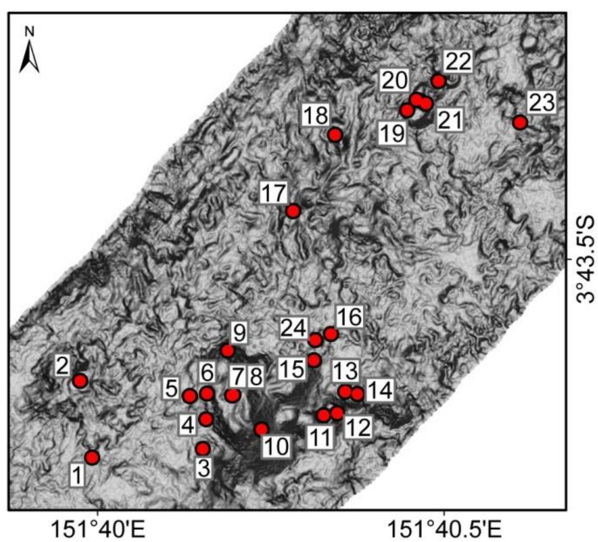

Vent Field Name (Coordinates)	Location	Depth of measurement [m] / Year	Max T [°C] / Year	Areal extent [m²]
Tsukushi (151.6667W / 3.7297S)	Oxide mounds	1660 / 2006 1665 / 2011	62 / 2006 53 / 2011	Total diffuse: 1792 Total chimneys: 1225
Snowcap (151.6693W / 3.7281S)	Cluster-1 Cluster-2 Cluster-3 Cluster-4	X (inactive) 1651 / 2006 1639 / 2006 1644 / 2011 1643 / 2006 1647 / 2011	X (inactive) 63 / 2006 179 / 2006 224 / 2011 151 / 2006 34 / 2011	10 60 66 10 Total chimneys: 146 Total diffuse: 3680
Fenway (151.6723W / 3.7286S)	Main field (diffuse) Big Papi Cluster-1 Cluster-2 Cluster-3 Cluster-4	1701 / 2006 1709 / 2011 1705 / 2006 1715 / 2011 1710 / 2006 1714 / 2011 X (partly active) X (inactive) X (inactive)	8 / 2006 14 / 2011 353 / 2006 304 / 2011 330 / 2006 313 / 2011 X (partly active) X (inactive) X (inactive)	3300 110 60 247 16 71 Total chimneys: 652 Total diffuse: 4450
Satanic Mills (151.672W / 3.7267S)	Central chimney cluster	1685 / 2006 1688 / 2011	295 / 2006 345 / 2011	314 Total chimneys: 564 Total diffuse: 690
Roman Ruins (151.6748W / 3.721S)	Main chimney field marginal active chimney cluster	1666 / 2006 1679 / 2011 X	316 / 2006 334 / 2011 X	6331 678 Total chimneys: 7709 Total diffuse: 135
Rogers Ruins (151.674W / 3.7191S)	Main field	1709 / 2006	320 / 2006	273 Total chimneys: 319 Total diffuse: 70
Solwara-6 (151.6801W / 3.7281S)	x	x	x	Total diffuse: 340
Solwara-7 (151.6728W / 3.7172S)		1774 / 2011	348 / 2011	Total chimneys: 229 Total diffuse: X
Solwara-8 (151.6742W / 3.7305S)	Main field	1740 / 2011	305 / 2011	330 m2 Total chimneys: 501 Total diffuse: X
Mimosa (151.6734W / 3.7293S)	x	x	x	Total chimneys: 120 Total diffuse: 240

Table S2: Summary of hydrothermal vent fields within the PACManus hydrothermal area. Listed are active chimney clusters and diffuse venting fields. Marginal, inactive chimney clusters not mentioned in this publication are included in the total area but not listed separately.